

KA-TP-1-2002
 UB-ECM-PF-02/03
 MPI-PhT/2002-27
 PSI-PR-02-07
 hep-ph/0207364

Fermionic decays of sfermions: a complete discussion at one-loop order

Jaume Guasch^{a,b}, Wolfgang Hollik^{a,c}, Joan Solà^{d,e}

^a *Institut für Theoretische Physik, Universität Karlsruhe, Kaiserstraße 12,
 D-76128 Karlsruhe, Germany*

^b *Theory Group LTP, Paul Scherrer Institut, CH-5232 Villigen PSI, Switzerland*

^c *Max-Planck-Institut für Physik, Föhringer Ring 6, D-80805 München, Germany*

^d *Departament d'Estructura i Constituents de la Matèria, Universitat de Barcelona,
 Diagonal 647, E-08028, Barcelona, Catalonia, Spain*

^e *Institut de Física d'Altes Energies, Universitat Autònoma de Barcelona, E-08193,
 Bellaterra, Barcelona, Catalonia, Spain*

Abstract

We present a definition of an on-shell renormalization scheme for the sfermion and chargino-neutralino sector of the Minimal Supersymmetric Standard Model (MSSM). Then, apply this renormalization framework to the interaction between charginos/neutralinos and sfermions. A kind of universal corrections is identified, which allow to define effective chargino/neutralino coupling matrices. In turn, these interactions generate (universal) non-decoupling terms that grow as the logarithm of the heavy mass. Therefore the full MSSM spectrum must be taken into account in the computation of radiative corrections to observables involving these interactions. As an application we analyze the full one-loop electroweak radiative corrections to the partial decay widths $\Gamma(\tilde{f} \rightarrow f\chi^0)$ and $\Gamma(\tilde{f} \rightarrow f'\chi^\pm)$ for all sfermion flavours and generations. These are combined with the QCD corrections to compute the corrected branching ratios of sfermions. It turns out that the electroweak corrections can have an important impact on the partial decay widths, as well as the branching ratios, in wide regions of the parameter space. The precise value of the corrections is strongly dependent on the correlation between the different particle masses.

1 Introduction

The Standard Model (SM) of the strong and electroweak interactions is the present paradigm of particle physics. Its validity has been tested to a level better than one per mille at particle accelerators [1]. Nevertheless, there are arguments against the SM being the fundamental model of particle interactions [2], giving rise to the investigation of competing alternative or extended models, which can be tested at high-energy colliders, such as the Large Hadron Collider (LHC) [3], or a e^+e^- Linear Collider (LC) [4]. One of the most promising possibilities for physics beyond the SM is the incorporation of Supersymmetry (SUSY), which leads to a renormalizable field theory with precisely calculable predictions to be tested in future experiments. The simplest supersymmetric extension of the SM is the Minimal Supersymmetric Standard Model (MSSM) [5]. Up to now the major effort on the computation of SUSY radiative corrections has been put into the computation of virtual SUSY effects in observables that involve only SM external particles, or into the calculation of loop effects in the extended Higgs sector of the MSSM¹. In this context, if the masses of the extra non-standard particles are very large as compared to the SM electroweak scale, the effects of these particles decouple, leaving the SM as a low-energy effective theory². This means that if the extra particles are too heavy we could not discern between the SM and the MSSM by just looking at the low-energy end of the spectrum, since the only trace of the MSSM would be a light Higgs boson ($M_{h^0} \lesssim 135$ GeV) [8], whose properties would not differ from the SM one. But for the case of direct production of SUSY particles, one also needs a detailed knowledge of the higher-order effects for the processes with these SUSY particles in the external states. In contrast to the case of virtual SUSY effects in SM Green's functions, there is a great variety of additional electroweak MSSM processes, viz. those involving Higgs bosons and/or (R-odd) sparticles in the external legs, for which the decoupling limit cannot be applied. In this case several kinds of non-decoupling effects may appear which grow with the mass of the sparticles [9, 10, 11, 12]. These effects can be very important, as they could provide the clue to discovering SUSY physics in the colliders. This was amply demonstrated in the past for decay processes [13, 14], and also very recently for production cross-sections in hadron colliders [15], in both cases exploiting the SUSY threshold corrections in the top quark and Higgs boson sector. In the present study, however, we will face not only threshold effects, but also a new type of non-decoupling (so-called universal) contributions. Both types of non-decoupling effects have to be considered for a complete study of sfermion decays in the colliders. The LHC will be able to discover new particles with masses up to 2.5 TeV. Provided they are not too heavy, the LC will be able to make precision measurements of their properties. For example, at a 500 GeV LC with a total integrated luminosity of 500 fb⁻¹ a measurement of the top-squark mass and the top-squark mixing angle can be performed with a precision of 0.5% and 1.5% respectively [16]. For an adequate analysis, precise theoretical predictions are required, going beyond the Born approximation. These studies of purely supersym-

¹See e.g. [6] and references therein.

²See e.g. [7] and references therein.

metric processes at the quantum level are necessary not only to refine the prediction of the corresponding observables but also because 1) the quantum corrections may severely affect the physical production of the supersymmetric particles, and 2) in addition they probe the underlying SUSY nature present in the model, that is: the relation between the gauge couplings of the SM gauge bosons and the Yukawa coupling of its SUSY partners (charginos and neutralinos). Beyond leading order this relation receives corrections which are non-decoupling.

A number of studies have already addressed this issue, for production as well as for decay processes. For squark and gluino production in hadron collisions, the NLO QCD corrections are available [17]; for squark-pair production in e^+e^- collisions, the NLO QCD are also known, together with the Yukawa corrections [18]. Concerning the subsequent squark decays into charginos/neutralinos, the QCD corrections were presented in [19, 11]³, whereas the Yukawa corrections were given in [21]⁴. In this last work large corrections were found. They were derived, however, in the *higgsino* approximation for the chargino; hence, a full computation is required to consolidate the significance of the loop effects.

We have performed a complete one-loop computation of the electroweak radiative corrections to the partial decay widths of sfermions into fermions and charginos/neutralinos,

$$\Gamma(\tilde{f} \rightarrow f'\chi) . \quad (1)$$

We present the structure of the corrections in detail, and illustrate their main features and their significance in representative numerical examples. Explicit results are displayed for all kind of sfermions. First results of this study were presented in Ref. [23].

In processes with exclusively SM particles in external states, it is possible to divide the one-loop contributions into SM-like and non-SM-like subclasses. This separate treatment is often used in the literature, and it is useful since it allows to make the computation in small steps, checking each sector individually. As a distinctive feature of the radiative corrections to processes with supersymmetric particles in the external legs, this separability is lost. In such kind of processes the ultraviolet (UV) divergences of diagrams with virtual SM particles cancel the UV divergences of diagrams with non-SM particles. Any partial computation would yield UV-divergent and thus meaningless results. For this reason we have to compute the entire set of one-loop contributions for our processes, with the proper counterterms involving the renormalization of almost the full MSSM Lagrangian. As a direct consequence, many non-decoupling effects appear. Moreover, we remark that since we have sparticles in the external legs a consistent calculation of the loop integrals requires the use of dimensional reduction in order that the regularization procedure preserves supersymmetry [24]⁵.

Section 2 contains the renormalization of the sfermion sector (section 2.2), the chargino/neutralino sector (section 2.3), and their interaction (section 2.4). The numerical

³The gluino decay channel, which can be overwhelming for $m_{\tilde{q}} > m_q + m_{\tilde{g}}$, was studied in [20]. Here we will assume $m_{\tilde{g}} > m_{\tilde{q}_a}$.

⁴A direct comparison between the QCD and the Yukawa corrections can be found in Ref. [22].

⁵One could also make use of a SUSY-breaking regularization, and introduce corresponding SUSY-breaking counterterms to restore supersymmetry at the one-loop order, see e.g. [25].

analysis is done in section 3, including the combination of the electroweak effects with the QCD ones, and the computation of the one-loop corrected branching ratios. Finally section 4 is devoted to the conclusions.

2 Renormalization and radiative corrections

2.1 Introduction

It is our aim to complement the on-shell scheme of the SM to include the SUSY particles. The renormalization of the SM is done according to Ref. [26] apart from some sign conventions. However, when extending this renormalization framework to embrace the whole MSSM we will treat the field renormalization of the supersymmetric particles in a different way that will be described at due point. The so-called α -scheme is used, in which the input parameters for the gauge sector are chosen to be the fine structure constant α (defined in the Thomson limit) and the pole masses of the weak gauge bosons M_W , M_Z . The electroweak mixing angle is defined on-shell:⁶ $s_W^2 = 1 - M_W^2/M_Z^2$.

The Higgs sector of the MSSM has received a lot of attention in the literature [8, 27, 28]. Here we follow Ref. [27]. In fact, the only ingredient of the Higgs sector needed at one-loop order for renormalization of the sfermion and the chargino-neutralino sectors is the renormalization of $\tan\beta$. The counterterm is determined by the condition for the counterterms of the two vacuum expectation values,

$$\frac{\delta v_1}{v_1} = \frac{\delta v_2}{v_2},$$

together with the absence of mixing between the on-shell A^0 Higgs boson and the Z weak gauge boson, which gives

$$\frac{\delta \tan\beta}{\tan\beta} = -\frac{1}{M_Z s_{2\beta}} \Sigma^{A^0 Z^0}(M_{A^0}^2).$$

Our choice of $\tan\beta$ is based on simplicity. It is known that all definitions of $\tan\beta$ not directly related to a physical observable are subject to some gauge dependence and/or induce large variations of the corrections with the parameters⁷. In our case the dependence is small and, with this simple and well tested definition, we can avoid introducing process-dependent corrections in a framework, like ours, which is already quite cumbersome. Needless to say, the physical observables we are addressing, like decay rates and branching ratios, are completely insensitive to our particular choice of $\tan\beta$.

⁶We abbreviate trigonometric functions by their initials, like $s_W \equiv \sin\theta_W$, $s_{2\beta} \equiv \sin(2\beta)$, $t_W = s_W/c_W$, etc.

⁷For a specific physical definition of $\tan\beta$, free of these problems, see e.g. Ref. [13]. As a drawback, however, one has to compute the process-dependent corrections. See also [29] for a recent review on this subject.

Besides parameter renormalization, we introduce field-renormalization constants for each particle. Exploiting the freedom in the treatment of field renormalization, they have been chosen in a way to get fairly simple expressions for the physical observables under study.

2.2 Sfermion sector

Throughout this paper we will be using the 3th family squarks as a generic fermion-sfermion notation. The same relations hold for sleptons, by changing the corresponding charges appropriately.

We denote the two sfermion-mass eigenvalues by $m_{\tilde{f}_a}$ ($a = 1, 2$), with $m_{\tilde{f}_1} > m_{\tilde{f}_2}$. The sfermion-mixing angle θ_f is defined by the transformation relating the weak-interaction ($\tilde{f}'_a = \tilde{f}_L, \tilde{f}_R$) and the mass eigenstate ($\tilde{f}_a = \tilde{f}_1, \tilde{f}_2$) sfermion bases:

$$\tilde{f}'_a = R_{ab}^{(f)} \tilde{f}_b ; \quad R^{(f)} = \begin{pmatrix} \cos \theta_f & -\sin \theta_f \\ \sin \theta_f & \cos \theta_f \end{pmatrix}. \quad (2)$$

By this basis transformation, the sfermion mass matrix,

$$\mathcal{M}_{\tilde{f}}^2 = \begin{pmatrix} M_{\tilde{f}_L}^2 + m_f^2 + c_{2\beta}(T_3 - Q s_W^2) M_Z^2 & m_f M_f^{LR} \\ m_f M_f^{LR} & M_{\tilde{f}_R}^2 + m_f^2 + Q c_{2\beta} s_W^2 M_Z^2 \end{pmatrix}, \quad (3)$$

becomes diagonal: $R^{(f)\dagger} \mathcal{M}_{\tilde{f}}^2 R^{(f)} = \text{diag} \{m_{\tilde{f}_1}^2, m_{\tilde{f}_2}^2\}$. $M_{\tilde{f}_L}^2$ is the soft-SUSY-breaking mass parameter of the $SU(2)_L$ doublet⁸, whereas $M_{\tilde{f}_R}^2$ is the soft-SUSY-breaking mass parameter of the singlet. T_3 and Q are the usual third component of the isospin and the electric charge respectively. The mixing parameters in the non-diagonal entries read

$$M_b^{LR} = A_b - \mu \tan \beta \quad , \quad M_t^{LR} = A_t - \mu / \tan \beta .$$

Our aim is to compute the radiative corrections in an on-shell renormalization scheme; hence, the input parameters are physical observables (i.e. the physical masses $m_{\tilde{b}_2}, m_{\tilde{b}_1}, \dots$) rather than formal parameters in the Lagrangian (i.e. the soft-SUSY-breaking parameters $M_{\tilde{b}_L}^2, A_b, \dots$ in eq. (3)). Specifically, we use the following set of independent parameters for the squark sector:

$$(m_{\tilde{b}_1}, m_{\tilde{b}_2}, \theta_b, m_{\tilde{t}_2}, \theta_t). \quad (4)$$

The value of the other stop mass, $m_{\tilde{t}_1}$, is derived from this set of input parameters. The sbottom and stop trilinear soft-SUSY-breaking terms A_b and A_t are fixed at the tree-level by the previous parameters as follows:

$$A_b = \mu \tan \beta + \frac{m_{\tilde{b}_1}^2 - m_{\tilde{b}_2}^2}{2 m_b} \sin 2 \theta_b ; \quad A_t = \mu \cot \beta + \frac{m_{\tilde{t}_1}^2 - m_{\tilde{t}_2}^2}{2 m_t} \sin 2 \theta_t . \quad (5)$$

⁸With $M_{\tilde{t}_L} = M_{\tilde{b}_L}$ due to $SU(2)_L$ gauge invariance.

We impose the approximate (necessary) condition

$$A_q^2 < 3(m_{\tilde{t}}^2 + m_{\tilde{b}}^2 + M_H^2 + \mu^2), \quad (6)$$

where $m_{\tilde{q}}$ is of the order of the average squark masses for $\tilde{q} = \tilde{t}, \tilde{b}$, to avoid colour-breaking minima in the MSSM Higgs potential [30]. Of course the relation (5) receives one-loop corrections; however, since these parameters do not enter the tree-level expressions, these effects translate into two-loop corrections to the process under study. The bound (6) translates into a stringent constraint to the sbottom-quark mixing angle for moderate and large values of $\tan \beta \gtrsim 10$: with an approximate limit $|\mu| \gtrsim 80$ GeV from the negative output of the chargino search at LEP, the condition (6) can only be satisfied by a cancellation of the two terms in (5) which is easily spoiled when θ_b is varied. However, the right hand side of eq. (6) is not rigorous [30]; so we will present results also when this bound is not satisfied, but we will clearly mark these regions. With the use of the bound (6) also the squark-squark-Higgs-boson couplings are restricted. This is a welcome feature, since these couplings can in general be very large, eventually spoiling perturbativity.

The slepton sector follows the same procedure, but only one sneutrino is present. Thus the input parameters in eq. (4) are reduced to the charged slepton masses and mixing angle.

The definition of the on-shell renormalization scheme is driven by the input parameters (4). The two bottom-squarks and the lightest top-squark are defined to be on-shell, whereas the heaviest top-squark mass receives quantum corrections. The mixing angle renormalization must also be given. Since there is no unique concept of an *on-shell angle*, a practical definition is given, which is general enough to be used in any sfermion observable.

Other definitions of an *on-shell* scheme are also conceivable. One could think, for example, of a concept having all the sfermions defined on-shell, so that the input parameters would be the four masses and one mixing angle. Such a scheme, however, is problematic. First of all, this input parameter set is not complete, and one needs to give also the sign of the angle to determine completely the parameters of the sfermion section. Second, the expression derived for the counterterm of the mixing angle is not well defined when the angle is zero (no mixing). Admittedly, the zero-mixing-angle case could be thought of as an academic limit; it is, however, a very useful scenario for the study of sfermions at colliders, and has widely been used accordingly. Therefore, a renormalization framework which permits a consistent treatment of the zero-mixing-angle limit is desirable.

This on-shell sfermion-sector renormalization was already introduced in [21]. Here we expand this renormalization framework to include the relation between bottom-squark and top-squark counterterms, and provide a thorough discussion.

For each squark type $a = 1, 2$ we introduce a set of field-renormalization constants as follows,

$$\tilde{f}_a^{(0)} = (Z_f^a)^{1/2} \tilde{f}_a + (1 - \delta^{ab}) \delta Z_f^{ab} \tilde{f}_b \quad , \quad (7)$$

where we have attached a superscript (0) to the bare fields, and δ^{ab} is the usual Kronecker delta. As for parameter renormalization, we introduce counterterms for each independent

parameter in eq. (4):

$$(m_{\tilde{b}_a}^2)^{(0)} \equiv m_{\tilde{b}_a}^2 + \delta m_{\tilde{b}_a}^2, \quad (m_{\tilde{t}_2}^2)^{(0)} \equiv m_{\tilde{t}_2}^2 + \delta m_{\tilde{t}_2}^2, \quad \theta_f^{(0)} \equiv \theta_f + \delta\theta_f. \quad (8)$$

The bare fields in the interaction basis are related to the bare fields in the mass basis as

$$(\tilde{f}')^{(0)} = R^{(f)(0)}(\tilde{f})^{(0)}, \quad R^{(f)(0)} \equiv R^{(f)} + \delta R^{(f)}, \quad \delta R_{ab}^{(f)} = \frac{\partial R_{ab}^{(f)}}{\partial \theta_f} \delta\theta_f. \quad (9)$$

The counterterms to the soft-SUSY-breaking parameters in eq. (3) can be found by

$$(\mathcal{M}_{\tilde{f}}^2)^{(0)} = R^{(f)(0)} \begin{pmatrix} (m_{\tilde{f}_1}^2)^{(0)} & 0 \\ 0 & (m_{\tilde{f}_2}^2)^{(0)} \end{pmatrix} (R^{(f)(0)})^\dagger. \quad (10)$$

The bottom-squarks and the lightest top-squark are defined to be on-shell, the residue of the renormalized propagators is taken to be 1 and we require no-mixing between the sfermions, that is⁹

$$\begin{aligned} \delta m_{\tilde{f}}^2 &= -\Sigma_{\tilde{f}}(m_{\tilde{f}}^2), \quad \tilde{f} = \tilde{b}_a, \tilde{t}_2, \\ \delta Z_{\tilde{f}}^a &= \Sigma'_{\tilde{f}_a}(m_{\tilde{f}_a}^2), \quad \tilde{f}_a = \tilde{b}_a, \tilde{t}_a, \\ \delta Z_{\tilde{f}}^{ab} &= \frac{\Sigma_{\tilde{f}}^{ab}(m_{\tilde{f}_b}^2)}{m_{\tilde{f}_b}^2 - m_{\tilde{f}_a}^2}, \quad \tilde{f} = \tilde{b}, \tilde{t}, \quad (a \neq b). \end{aligned} \quad (11)$$

The mixing angles in the sfermion sector do not receive radiative corrections. The corresponding counterterm is fixed by means of the non-diagonal field-renormalization constants of eq. (7) as follows:

$$\delta\theta_f = \frac{1}{2} (\delta Z_{\tilde{f}}^{12} - \delta Z_{\tilde{f}}^{21}) = \frac{1}{2} \frac{\Sigma_{\tilde{f}}^{12}(m_{\tilde{f}_2}^2) + \Sigma_{\tilde{f}}^{12}(m_{\tilde{f}_1}^2)}{m_{\tilde{f}_2}^2 - m_{\tilde{f}_1}^2}. \quad (12)$$

The set of equations (11), (12) defines all the counterterms in the sfermion sector. The one-loop electroweak Feynman diagrams contributing to the sfermions self-energies are shown schematically in Fig. 1a.

The heaviest top-squark is not defined on-shell, and therefore its mass receives radiative corrections. In order to find them we make use of eq. (10). Since the bottom-squarks are defined to be on-shell, the counterterm to the soft-SUSY-breaking squared mass $M_{\tilde{b}_L}^2$ is found to be

$$\delta M_{\tilde{b}_L}^2 = \delta(\mathcal{M}_{\tilde{b}}^2)_{11} - 2m_b \delta m_b - c_{2\beta}(T_3^b - Q^b s_W^2) \delta M_Z^2 - M_Z^2 \left(\delta c_{2\beta}(T_3^b - Q^b s_W^2) - c_{2\beta} Q^b \delta s_W^2 \right), \quad (13)$$

which is used in the top-squark matrix

$$\delta(\mathcal{M}_{\tilde{t}}^2)_{11} = \delta M_{\tilde{b}_L}^2 + 2m_t \delta m_t + c_{2\beta}(T_3^t - Q^t s_W^2) \delta M_Z^2 + M_Z^2 \left(\delta c_{2\beta}(T_3^t - Q^t s_W^2) - c_{2\beta} Q^t \delta s_W^2 \right). \quad (14)$$

⁹It is understood that only the real part of the self-energies is taken in the counterterm definitions.

The fermion mass-counterterms $\delta m_b, \delta m_t$ are computed with the help of the Feynman diagrams of Fig. 1b. With these results, the counterterm for the \tilde{t}_1 mass is found to be

$$\delta m_{\tilde{t}_1}^2 = \frac{1}{(R_{11}^{(t)})^2} \left(\delta(\mathcal{M}_{\tilde{t}}^2)_{11} - (R_{21}^{(t)})^2 \delta m_{\tilde{t}_2}^2 - 2m_{\tilde{t}_1}^2 R_{11}^{(t)} \delta R_{11}^{(t)} - 2m_{\tilde{t}_2}^2 R_{12}^{(t)} \delta R_{12}^{(t)} \right). \quad (15)$$

Note that this renormalization prescription breaks down for $\theta_t = \pi/2$. In this case we have that $\tilde{t}_1 = \tilde{t}_R$, whose mass is not related to the bottom-squark; then it would be better to use a renormalization prescription where $m_{\tilde{t}_1}$ is the input parameter. Of course, this renormalization prescription would break down in turn at $\theta_t = 0$.

The one-loop on-shell mass for the \tilde{t}_1 is then given by

$$(m_{\tilde{t}_1}^2)^{\text{os}} = (m_{\tilde{t}_1}^2)^{\text{tree}} + \delta m_{\tilde{t}_1}^2 + \Sigma_{\tilde{t}_1}(m_{\tilde{t}_1}^2). \quad (16)$$

In Section 3 we give numerical values for the correction to the top-squark mass.

2.3 Chargino-neutralino sector

This sector contains six particle masses, but only three free parameters are available for an independent renormalization. As a consequence, we are not allowed to impose on-shell conditions for all the particle masses. For the independent input parameters, we choose: the masses of the two charginos and the mass of the lightest neutralino,

$$(M_1, M_2, M_1^0). \quad (17)$$

Although the tree-level chargino-neutralino sector is well known, we give here a short description, in order to set our conventions. We start by constructing the following set of Weyl spinors:

$$\begin{aligned} \Gamma^+ &\equiv (-i\tilde{W}^+, \tilde{H}_2^+) , \\ \Gamma^- &\equiv (-i\tilde{W}^-, \tilde{H}_1^-) , \\ \Gamma^0 &\equiv (-i\tilde{B}^0, -i\tilde{W}_3^0, \tilde{H}_1^0, \tilde{H}_2^0) . \end{aligned} \quad (18)$$

The mass Lagrangian in this basis reads

$$\mathcal{L}_M = -\frac{1}{2} (\Gamma^+, \Gamma^-) \begin{pmatrix} 0 & \mathcal{M}^T \\ \mathcal{M} & 0 \end{pmatrix} \begin{pmatrix} \Gamma^+ \\ \Gamma^- \end{pmatrix} - \frac{1}{2} (\Gamma_1, \Gamma_2, \Gamma_3, \Gamma_4) \mathcal{M}^0 \begin{pmatrix} \Gamma_1 \\ \Gamma_2 \\ \Gamma_3 \\ \Gamma_4 \end{pmatrix} + \text{h.c.} , \quad (19)$$

where we have defined

$$\begin{aligned} \mathcal{M} &= \begin{pmatrix} M & \sqrt{2}M_W s_\beta \\ \sqrt{2}M_W c_\beta & \mu \end{pmatrix} , \\ \mathcal{M}^0 &= \begin{pmatrix} M' & 0 & M_Z c_\beta s_W & -M_Z s_\beta s_W \\ 0 & M & -M_Z c_\beta c_W & M_Z s_\beta c_W \\ M_Z c_\beta s_W & -M_Z c_\beta c_W & 0 & -\mu \\ -M_Z s_\beta s_W & M_Z s_\beta c_W & -\mu & 0 \end{pmatrix} , \end{aligned} \quad (20)$$

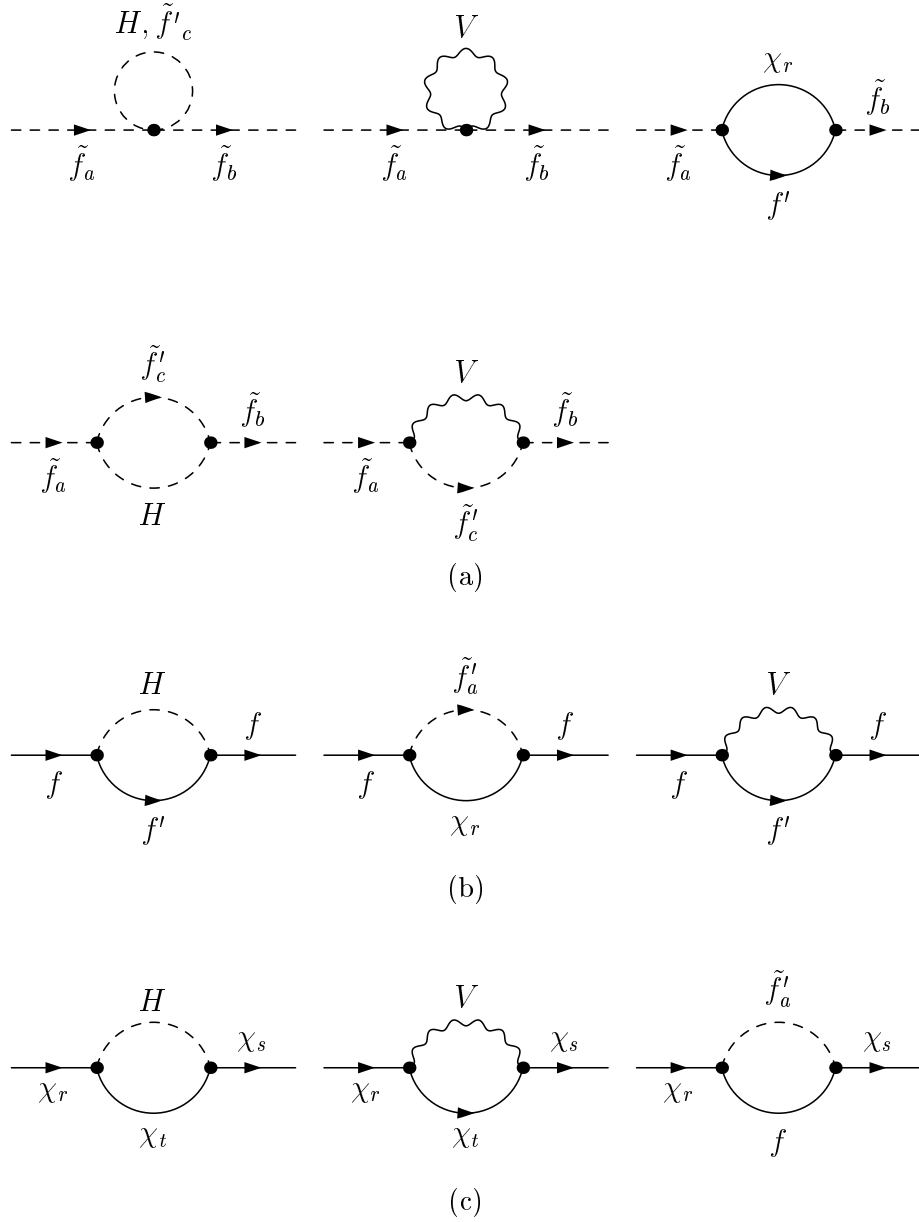


Figure 1: Generic electroweak one-loop diagrams contributing to the direct and mixed self-energies of **a)** sfermions; **b)** SM fermions; **c)** charginos/neutralinos. \tilde{f}_a stands for sfermions, f for SM fermions, χ_r for charginos or neutralinos, H for scalar particles (Higgs or Goldstone bosons), V for electroweak gauge bosons.

with M and M' the $SU(2)_L$ and $U(1)_Y$ soft-SUSY-breaking gaugino masses. The four-component mass-eigenstate fields are related to the ones in (18) by

$$\chi_i^+ = \begin{pmatrix} V_{ij}\Gamma_j^+ \\ U_{ij}^*\bar{\Gamma}_j^- \end{pmatrix} \quad , \quad \chi_i^- = \mathcal{C}\bar{\chi}_i^{+T} = \begin{pmatrix} U_{ij}\Gamma_j^- \\ V_{ij}^*\bar{\Gamma}_j^+ \end{pmatrix} \quad , \quad \chi_\alpha^0 = \begin{pmatrix} N_{\alpha\beta}\Gamma_\beta^0 \\ N_{\alpha\beta}^*\bar{\Gamma}_\beta^0 \end{pmatrix} = \mathcal{C}\bar{\chi}_\alpha^{0T} \quad , \quad (21)$$

where U , V and N are in general complex matrices that diagonalize the mass-matrices (20):

$$\begin{aligned} U^*\mathcal{M}V^\dagger &= \mathcal{M}_D = \text{diag}(M_1, M_2) \quad (0 < M_1 < M_2) \quad , \\ N^*\mathcal{M}^0N^\dagger &= \mathcal{M}_D^0 = \text{diag}(M_1^0, M_2^0, M_3^0, M_4^0) \quad (0 < M_1^0 < M_2^0 < M_3^0 < M_4^0) \quad . \end{aligned} \quad (22)$$

The renormalization framework is as follows: we introduce the renormalization constants for each parameter in the mass matrices (20). The counterterms δM_Z , δM_W , δc_W and $\delta \tan \beta$ are fixed from the conditions on the gauge and Higgs sectors of the theory, and we must provide renormalization prescriptions for δM , $\delta \mu$ and $\delta M'$. The mixing matrices U , V and N are defined to diagonalize the renormalized mass matrices. The bare mass Lagrangian is then

$$\mathcal{L}_M^{(0)} = -(\bar{\chi}^-)^{(0)} (M_D + \delta M_D) (\chi^-)^{(0)} - \frac{1}{2}(\bar{\chi}^0)^{(0)} (M_D^0 + \delta M_D^0) (\chi^0)^{(0)} \quad (23)$$

with

$$\delta M_D = U^*\delta\mathcal{M}V^\dagger \quad , \quad \delta M_D^0 = N^*\delta\mathcal{M}^0N^\dagger \quad .$$

Note that these counterterm matrices are non-diagonal. This renormalization corresponds to the following relation between the bare weak- and mass-eigenstates fields:

$$(\chi_i^-)^{(0)} = \begin{pmatrix} U_{ij}(\Gamma_j^-)^{(0)} \\ V_{ij}^*(\bar{\Gamma}_j^+)^{(0)} \end{pmatrix} \quad , \quad (\chi_\alpha^0)^{(0)} = \begin{pmatrix} N_{\alpha\beta}(\Gamma_\beta^0)^{(0)} \\ N_{\alpha\beta}^*(\bar{\Gamma}_\beta^0)^{(0)} \end{pmatrix} \quad . \quad (24)$$

Note that no counterterms for the mixing matrices are introduced. As far as field renormalization is concerned, we introduce different field-renormalization constants for each chargino and neutralino:

$$(\chi_s)^{(0)} \equiv \chi_s + \frac{1}{2}\delta Z_L^s P_L \chi_s + \frac{1}{2}\delta Z_R^s P_R \chi_s \quad , \quad \chi_s \equiv \chi_i^\pm, \chi_\alpha^0 \quad , \quad (25)$$

with the chirality projectors $P_{\{L,R\}} = 1 \mp \gamma_5$. The renormalization framework is thus complete¹⁰. Now we must supply renormalization conditions for each parameter in eq. (17) and wave-function renormalization constant. We will fix δM and $\delta \mu$ by requiring that the one-loop renormalized chargino masses are the on-shell masses. $\delta M'$ is fixed by requiring that the lightest renormalized neutralino mass is the on-shell mass. The wave-function renormalization constants are fixed by requiring that the renormalized propagator has residue one.

¹⁰One can take either the χ^+ or the χ^- to perform the renormalization. We will take the self-energies and the corresponding renormalization constants to be that of the χ^- . One has, evidently, $\delta Z_L^{-i} = \delta Z_R^{+i}$ and $\delta Z_L^{+i} = \delta Z_R^{-i}$.

Using this framework, we are able to relate the counterterms of the fundamental parameters to the mass-counterterms δM_i of the charginos. Similarly to [31] we find:

$$\begin{aligned} M_1 \delta M_1 + M_2 \delta M_2 &= M \delta M + \mu \delta \mu + \delta M_W^2, \\ M_1 M_2 (M_1 \delta M_2 + M_2 \delta M_1) &= \left(M \mu - M_W^2 s_{2\beta} \right) \left[M \delta \mu + \mu \delta M \right. \\ &\quad \left. - M_W^2 \delta s_{2\beta} - s_{2\beta} \delta M_W^2 \right]. \end{aligned} \quad (26)$$

The mass counterterms δM_i are fixed using the on-shell scheme relation, in the convention of [26] (but with opposite sign for Σ),

$$\frac{\delta M_i}{M_i} = -\frac{1}{2} \left(\Sigma_L^{-i}(M_i^2) + \Sigma_R^{-i}(M_i^2) \right) - \Sigma_S^{-i}(M_i^2), \quad (27)$$

where $\Sigma_{\{L,R,S\}}^i$ denote the one-loop unrenormalized left-, right-handed and scalar components of the self-energy for the i th-chargino. The wave function renormalization constants are

$$\delta Z_{L,R}^{-i} = \Sigma_{L,R}^{-i}(M_i^2) + M_i^2 [\Sigma_L^{-i'}(M_i^2) + \Sigma_R^{-i'}(M_i^2) + 2 \Sigma_S^{-i'}(M_i^2)]. \quad (28)$$

The one-loop diagrams contributing to the chargino/neutralino self-energies are shown schematically in Fig. 1c.

By solving the equations (26) we find the counterterms of the independent mass parameters of the chargino mass matrix (20):

$$\begin{aligned} \delta M &= \frac{M X_1 - \mu X_2}{M^2 - \mu^2}, \quad \delta \mu = \frac{\mu X_1 - M X_2}{\mu^2 - M^2}, \\ X_1 &= M_1 \delta M_1 + M_2 \delta M_2 - \delta M_W^2, \\ X_2 &= \frac{M \mu - M_W^2 s_{2\beta}}{M_1 M_2} (M_1 \delta M_2 + M_2 \delta M_1) + M_W^2 \delta s_{2\beta} + s_{2\beta} \delta M_W^2. \end{aligned} \quad (29)$$

$\delta M'$ is determined from the lightest neutralino mass, inverting the relation

$$N_{1\alpha}^* \delta \mathcal{M}_{\alpha\beta}^0 N_{1\beta}^* = \delta M_1^0, \quad (30)$$

where the neutralino-mass counterterm δM_1^0 is fixed by the on-shell condition for χ_1^0 , in analogy to (27). The result is then

$$\delta M' = \frac{1}{N_{11}^{*2}} \left(\delta M_1^0 - \sum_{\alpha \text{ or } \beta \neq 1} N_{1\alpha}^* \delta \mathcal{M}_{\alpha\beta}^0 N_{1\beta}^* \right). \quad (31)$$

It is a non-trivial check that with the counterterms determined in eqs. (26) and (30), the one-loop masses for the remaining neutralinos, computed as the pole masses, are UV-finite. The one-loop on-shell neutralino masses read

$$M_\alpha^{0 \text{ os}} = M_\alpha^0 + N_{\alpha\beta}^* \delta \mathcal{M}_{\beta\gamma}^0 N_{\alpha\gamma}^* + M_\alpha^0 \left\{ \frac{1}{2} \left(\Sigma_L^\alpha(M_\alpha^{02}) + \Sigma_R^\alpha(M_\alpha^{02}) \right) + \Sigma_S^\alpha(M_\alpha^{02}) \right\}, \quad (32)$$

where now the parameters of eq. (20) and the masses and mixing matrices computed in (22) have to be regarded as *renormalized* quantities.

The choice of the lightest neutralino to fix the counterterm $\delta M'$ in (30) is only efficient if it has a substantial *bino* component. If $M' \gg (|\mu|, M)$ then $|N_{11}| \ll 1$, and the extraction of $\delta M'$ from (31) would amplify the radiative corrections artificially. In this case it would be better to extract $\delta M'$ from the α th neutralino, such that $|N_{1\alpha}|$ is large. This is, however, not relevant for the scenarios which are discussed in this work. Notice also that our renormalization procedure makes use of positive-definite mass eigenvalues for charginos and neutralinos, which require the introduction of some purely-imaginary non-zero elements in the N -matrix (22). Had we chosen a real N -matrix, with some negative eigenvalues, the various renormalization conditions would be plagued with the explicit sign of the corresponding eigenvalue (see e.g. [32]).

At one-loop, also mixing self-energies between the different neutralinos and charginos are generated, which we write as follows:

$$-i\hat{\Sigma}^{\alpha\beta}(k^2) = -i\left(\hat{\Sigma}_L^{\alpha\beta}(k^2)\not{k}P_L + \hat{\Sigma}_R^{\alpha\beta}(k^2)\not{k}P_R + \hat{\Sigma}_{SL}^{\alpha\beta}(k^2)P_L + \hat{\Sigma}_{SR}^{\alpha\beta}(k^2)P_R\right), \quad \alpha \neq \beta, \quad (33)$$

with $\hat{\Sigma}$ denoting the renormalized two-point functions. For the neutralinos, the renormalized self-energies (33) are related to the unrenormalized ones according to

$$\hat{\Sigma}_{\{L,R\}}^{\alpha\beta} = \Sigma_{\{L,R\}}^{\alpha\beta}, \quad \hat{\Sigma}_{SL}^{\alpha\beta} = \Sigma_{SL}^{\alpha\beta} - N_{\alpha\gamma}\delta\mathcal{M}_{\gamma\lambda}^{0*}N_{\beta\lambda}, \quad \hat{\Sigma}_{SR}^{\alpha\beta} = \Sigma_{SR}^{\alpha\beta} - N_{\alpha\gamma}^*\delta\mathcal{M}_{\gamma\lambda}^0N_{\beta\lambda}^*. \quad (34)$$

Analogous expressions hold for the χ^- charginos, replacing $(\alpha\beta) \rightarrow (ij)$ in eq. (33), the renormalized χ^- chargino self-energies being given by

$$\hat{\Sigma}_{\{L,R\}}^{-ij} = \Sigma_{\{L,R\}}^{-ij}, \quad \hat{\Sigma}_{SL}^{-ij} = \Sigma_{SL}^{-ij} - U_{ik}^*\delta\mathcal{M}_{kl}V_{jl}^*, \quad \hat{\Sigma}_{SR}^{-ij} = \Sigma_{SR}^{-ij} - V_{ik}\delta\mathcal{M}_{lk}U_{lj}. \quad (35)$$

The one-loop mixing self-energies also contribute to the chargino and neutralino masses; their contribution is, however, of higher order in perturbation theory, and we do not take it into account in the mass spectrum.

The contribution of these mixing self-energies to the one-loop decay form factors can be written as follows. If \tilde{T}_α is the amputated one-particle irreducible 3-point Green's function for the creation of a χ_α^0 (represented by a spinor v_α), the full one-loop process amplitude reads:

$$T_\alpha = \bar{u}\tilde{T}_\alpha v_\alpha + \sum_{\beta \neq \alpha} \bar{u}\tilde{T}_\beta (\mathcal{Z}_L^{0\beta\alpha}P_L + \mathcal{Z}_R^{0\beta\alpha}P_R)v_\alpha, \quad (36)$$

where the external mixing wave function factors are

$$\begin{aligned} \mathcal{Z}_R^{0\beta\alpha} &= \frac{M_\beta^0 \hat{\Sigma}_{SL}^{\beta\alpha}(M_\alpha^{02}) + M_\alpha^0 \hat{\Sigma}_{SR}^{\beta\alpha}(M_\alpha^{02}) + M_\beta^0 M_\alpha^0 \hat{\Sigma}_L^{\beta\alpha}(M_\alpha^{02}) + M_\alpha^{02} \hat{\Sigma}_R^{\beta\alpha}(M_\alpha^{02})}{M_\alpha^{02} - M_\beta^{02}}, \\ \mathcal{Z}_L^{0\beta\alpha} &= \frac{M_\beta^0 \hat{\Sigma}_{SR}^{\beta\alpha}(M_\alpha^{02}) + M_\alpha^0 \hat{\Sigma}_{SL}^{\beta\alpha}(M_\alpha^{02}) + M_\beta^0 M_\alpha^0 \hat{\Sigma}_R^{\beta\alpha}(M_\alpha^{02}) + M_\alpha^{02} \hat{\Sigma}_L^{\beta\alpha}(M_\alpha^{02})}{M_\alpha^{02} - M_\beta^{02}}. \end{aligned} \quad (37)$$

The same expression is valid for the creation of a χ_i^+ (anti- χ_i^- , using $\mathcal{Z}_{L,R}^{-ji}$) changing the indices $\alpha \rightarrow i, \beta \rightarrow j$.¹¹

Admittedly, the choice of the two masses as input parameters is not ideal. For each pair of on-shell masses M_1, M_2 there exists up to a fourth-fold discrete ambiguity in the determination of the underlying parameters M and μ . There are, however, ways to determine uniquely these parameters. For example, assuming one knows both masses, either from a threshold scan in a LC or from the LHC, one can measure at the LC the production cross-section $\sigma(e^-e^+ \rightarrow \chi_1^-\chi_1^+)$ with different polarizations of the initial state electron and positron [33]. One finds in this way experimental values for the mixing matrix elements U_{ij}^{exp} and V_{ij}^{exp} which disentangle the ambiguity. One uses then the derived M and μ parameters to compute the renormalized U and V matrices, which are used for the computation of the radiative corrections.

A comment is in order regarding other renormalization prescriptions. Note that, at variance with Ref. [34, 35], our renormalization prescription does not introduce counterterms for the mixing matrices U, V and N . One can, in fact, introduce these counterterms and fix them in different ways. For example one could take the point of view that the mixing matrices are functions of the parameters in the mass matrix:

$$U = F_1(M, \mu, M_W, \tan \beta) \ , \ V = F_2(M, \mu, M_W, \tan \beta) \ , \ N = F_3(M', M, M_W, M_Z, \tan \beta) \ ,$$

and then one computes the counterterms as functions of the counterterms of the mass matrix:

$$\begin{aligned} \delta U &= f_1(\delta M, \delta \mu, \delta M_W, \delta \tan \beta) \ , \\ \delta V &= f_2(\delta M, \delta \mu, \delta M_W, \delta \tan \beta) \ , \\ \delta N &= f_3(\delta M', \delta M, \delta M_W, \delta M_Z, \delta \tan \beta) \ . \end{aligned}$$

The problem with this approach is that, while the analytic form of the chargino functions F_1 and F_2 are known, the neutralino function F_3 is usually computed numerically, and then the computation of f_3 is not possible. We have checked that this renormalization framework gives exactly the same results as the non-introduction of mixing matrix counterterms for the one-loop partial decay widths of sfermions into charginos. The authors of Ref. [34] take a different approach, introducing independent renormalization conditions for the counterterms of the mixing matrices. In Ref. [35] the counterterms to the U, V and N matrices are related to those of the mixing self-energies¹². When comparing the results presented here with the ones of Ref. [34, 35], one should therefore take into account that the meaning of the renormalized parameters M, μ, M' (and the mixing matrices) is not the same. When comparing physical quantities (such as pole masses), the results should be equivalent at one-loop order.

¹¹ The corresponding ones for χ_i^- (anti- χ_i^+) are $\mathcal{Z}_L^{+ji} \equiv \mathcal{Z}_R^{-ji}, \mathcal{Z}_R^{+ji} \equiv \mathcal{Z}_L^{-ji}$.

¹²See Ref. [35] for a comparison of the different renormalization schemes.

2.4 Vertex renormalization and decay amplitudes

Using the notation introduced in the above sections, the tree-level interaction Lagrangian between fermion-sfermion-(chargino or neutralino) reads [13]¹³

$$\begin{aligned}\mathcal{L}_{\chi\tilde{f}f'} &= \sum_{a=1,2} \sum_r \mathcal{L}_{\chi_r\tilde{f}_a f'} + \text{h.c.} , \\ \mathcal{L}_{\chi_r\tilde{f}_a f'} &= -g\tilde{f}_a^* \bar{\chi}_r \left(A_{+ar}^{(f)} P_L + A_{-ar}^{(f)} P_L \right) f' .\end{aligned}\tag{38}$$

Here we have adopted a compact notation, where f' is either f or its $SU(2)_L$ partner for χ_r being a neutralino or a chargino, respectively. Roman characters a, b, \dots are reserved for sfermion indices and i, j, \dots for chargino indices; Greek indices α, β, \dots denote neutralinos; Roman indices r, s, \dots indicate either a chargino or a neutralino. For example, the top-squark interactions with charginos are obtained by replacing $f \rightarrow t$, $f' \rightarrow b$, $\chi_r \rightarrow \chi_r^-$, $r = 1, 2$. The coupling matrices that encode the dynamics are given by

$$\begin{aligned}A_{+ai}^{(t)} &= R_{1a}^{(t)} V_{i1}^* - \lambda_t R_{2a}^{(t)} V_{i2}^* , \\ A_{-ai}^{(t)} &= -\lambda_b R_{1a}^{(t)} U_{i2} , \\ A_{+a\alpha}^{(t)} &= \frac{1}{\sqrt{2}} \left(R_{1a}^{(t)} (N_{\alpha 2}^* + Y_L t_W N_{\alpha 1}^*) + \sqrt{2} \lambda_t R_{2a}^{(t)} N_{\alpha 4}^* \right) , \\ A_{-a\alpha}^{(t)} &= \frac{1}{\sqrt{2}} \left(\sqrt{2} \lambda_t R_{1a}^{(t)} N_{\alpha 4} - Y_R^t t_W R_{2a}^{(t)} N_{\alpha 1} \right) , \\ A_{+ai}^{(b)} &= R_{1a}^{(b)} U_{i1}^* - \lambda_b R_{2a}^{(b)} U_{i2}^* , \\ A_{-ai}^{(b)} &= -\lambda_t R_{1a}^{(b)} V_{i2} , \\ A_{+a\alpha}^{(b)} &= -\frac{1}{\sqrt{2}} \left(R_{1a}^{(b)} (N_{\alpha 2}^* - Y_L t_W N_{\alpha 1}^*) - \sqrt{2} \lambda_b R_{2a}^{(b)} N_{\alpha 3}^* \right) , \\ A_{-a\alpha}^{(b)} &= -\frac{1}{\sqrt{2}} \left(-\sqrt{2} \lambda_b R_{1a}^{(b)} N_{\alpha 3} + Y_R^b t_W R_{2a}^{(b)} N_{\alpha 1} \right) ,\end{aligned}\tag{39}$$

with Y_L and $Y_R^{t,b}$ the weak hypercharges of the left-handed $SU(2)_L$ doublet and right-handed singlet fermion, and $\lambda_t = m_t/(\sqrt{2}M_W \sin \beta)$ and $\lambda_b = m_b/(\sqrt{2}M_W \cos \beta)$ are the Yukawa couplings normalized to the $SU(2)_L$ gauge coupling constant g .

As far as vertex renormalization is concerned, the vertex counterterms are already determined by the renormalization procedure described above. Introducing the one-loop counterterms analogously to [21] we obtain the following counterterm Lagrangian [21, 13]

$$\begin{aligned}\delta\mathcal{L}_{\chi_r\tilde{f}_a f'} &\equiv g\tilde{f}_a^* \bar{\chi}_r \left(\delta\Lambda_{+ar}^{(f)} P_L + \delta\Lambda_{-ar}^{(f)} P_R \right) f' + \text{h.c.} \\ &= \frac{1}{2} \left\{ \left[\frac{\delta\alpha}{\alpha} + \frac{c_W^2}{s_W^2} \left(\frac{\delta M_W^2}{M_W^2} - \frac{\delta M_Z^2}{M_Z^2} \right) \right] + \delta Z_{\tilde{f}}^a \right\} \mathcal{L}_{\chi_r\tilde{f}_a f'} + \mathcal{L}_{\chi_r\tilde{f}_b f'} \delta Z_{\tilde{f}}^{ba}\end{aligned}$$

¹³Note, however, a change of conventions, in the neutralino mass-matrices (20), and in the neutralino couplings. The change in the couplings allows for a joint presentation of the chargino and neutralino expressions.

$$\begin{aligned}
& + \left\{ g \tilde{f}_a^* \bar{\chi}_r \left[A_{+ar}^{(f)} \frac{1}{2} (\delta Z_R^r + \delta Z_L^f) P_L + A_{-ar}^{(f)} \frac{1}{2} (\delta Z_L^r + \delta Z_R^f) P_R \right] f' \right. \\
& \left. + g \tilde{f}_a^* \bar{\chi}_r (\delta A_{+ar}^{(f)} P_L + \delta A_{-ar}^{(f)} P_R) f' + \text{h.c.} \right\}, \quad (b \neq a), \\
\delta A_{+ai}^{(t)} &= \delta R_{1a}^{(t)} V_{i1}^* - (\lambda_t \delta R_{2a}^{(t)} + \delta \lambda_t R_{2a}^{(t)}) V_{i2}^*, \\
\delta A_{-ai}^{(t)} &= -(\lambda_b \delta R_{1a}^{(t)} + R_{1a}^{(t)} \delta \lambda_b) U_{i2}, \\
\delta A_{+a\alpha}^{(t)} &= \frac{1}{\sqrt{2}} (\delta R_{1a}^{(t)} (N_{\alpha 2}^* + Y_L t_W N_{\alpha 1}^*) + R_{1a}^{(t)} Y_L N_{\alpha 1}^* \delta t_W + \sqrt{2} (\lambda_t \delta R_{2a}^{(t)} + R_{2a}^{(t)} \delta \lambda_t) N_{\alpha 4}^*), \\
\delta A_{-a\alpha}^{(t)} &= \frac{1}{\sqrt{2}} (\sqrt{2} (\lambda_t \delta R_{1a}^{(t)} + R_{1a}^{(t)} \delta \lambda_t) N_{\alpha 4} - Y_R^t (t_W \delta R_{2a}^{(t)} + R_{2a}^{(t)} \delta t_W) N_{\alpha 1}), \\
\delta A_{+ai}^{(b)} &= \delta R_{1a}^{(b)} U_{i1}^* - (\lambda_b \delta R_{2a}^{(b)} + R_{2a}^{(b)} \delta \lambda_b) U_{i2}^*, \\
\delta A_{-ai}^{(b)} &= -(\lambda_t \delta R_{1a}^{(b)} + R_{1a}^{(b)} \delta \lambda_t) V_{i2}, \\
\delta A_{+a\alpha}^{(b)} &= -\frac{1}{\sqrt{2}} (\delta R_{1a}^{(b)} (N_{\alpha 2}^* - Y_L t_W N_{\alpha 1}^*) - R_{1a}^{(b)} Y_L N_{\alpha 1}^* \delta t_W - \sqrt{2} (\lambda_b \delta R_{2a}^{(b)} + R_{2a}^{(b)} \delta \lambda_b) N_{\alpha 3}^*), \\
\delta A_{-a\alpha}^{(b)} &= -\frac{1}{\sqrt{2}} (-\sqrt{2} (\lambda_b \delta R_{1a}^{(b)} + R_{1a}^{(b)} \delta \lambda_b) N_{\alpha 3} + Y_R^b (t_W \delta R_{2a}^{(b)} + R_{2a}^{(b)} \delta t_W) N_{\alpha 1}). \\
\frac{\delta \lambda_b}{\lambda_b} &= \frac{\delta m_b}{m_b} - \frac{1}{2} \frac{\delta M_W^2}{M_W^2} - \frac{\delta \cos \beta}{\cos \beta}, \quad \frac{\delta \lambda_t}{\lambda_t} = \frac{\delta m_t}{m_t} - \frac{1}{2} \frac{\delta M_W^2}{M_W^2} - \frac{\delta \sin \beta}{\sin \beta}, \\
\delta t_W &= \frac{1}{2s_W c_W} \left(\frac{\delta M_Z^2}{M_Z^2} - \frac{\delta M_W^2}{M_W^2} \right), \tag{40}
\end{aligned}$$

where $\delta\alpha$, $\delta M_{W,Z}^2$ are the charge and mass counterterms for the MSSM, as given in [36], and the counterterms for the mixing matrices have been defined in eq. (9).

The renormalized amplitude for the decay $\tilde{f}_a \rightarrow f' \chi_r$ can then be written at the one-loop level as follows,

$$\begin{aligned}
-iT_{ar} &\equiv -iT(\tilde{f}_a \rightarrow f' \chi_r) = -iT_{ar}^{\text{tree}} - iT_{ar}^{\text{loop}}, \\
-iT_{ar}^{\text{tree}} &= ig \bar{u}_{f'} [A_{+ar}^{(f)*} P_R + A_{-ar}^{(f)*} P_L] v_{\chi_r}, \\
-iT_{ar}^{\text{loop}} &= ig \bar{u}_{f'} [C_{+ar}^{(f)} P_R + C_{-ar}^{(f)} P_L] v_{\chi_r}; \quad C_{\pm ar}^{(f)} = \delta \Lambda_{\pm ar}^{(f)*} + \Lambda_{\pm ar}^{(f)\Sigma} + \Lambda_{\pm ar}^{(f)1\text{PI}}. \tag{41}
\end{aligned}$$

It contains, besides the counterterms $\delta\Lambda$ from (40), the one-loop contributions $\Lambda^{1\text{PI}}$ to the one-particle-irreducible three-point vertex functions shown in Fig. 2a, and the quantities Λ^Σ corresponding to the higher-order terms from the two-point functions in the one-loop expansion of the general expression (36), explicitly given by

$$\Lambda_{+ar}^{(f)\Sigma} = \sum_{s \neq r} A_{+as}^{(f)*} \mathcal{Z}_R^{sr}, \quad \Lambda_{-ar}^{(f)\Sigma} = \sum_{s \neq r} A_{-as}^{(f)*} \mathcal{Z}_L^{sr}, \tag{42}$$

where $\mathcal{Z}_{\{L,R\}}^{sr}$ has been defined in (37).

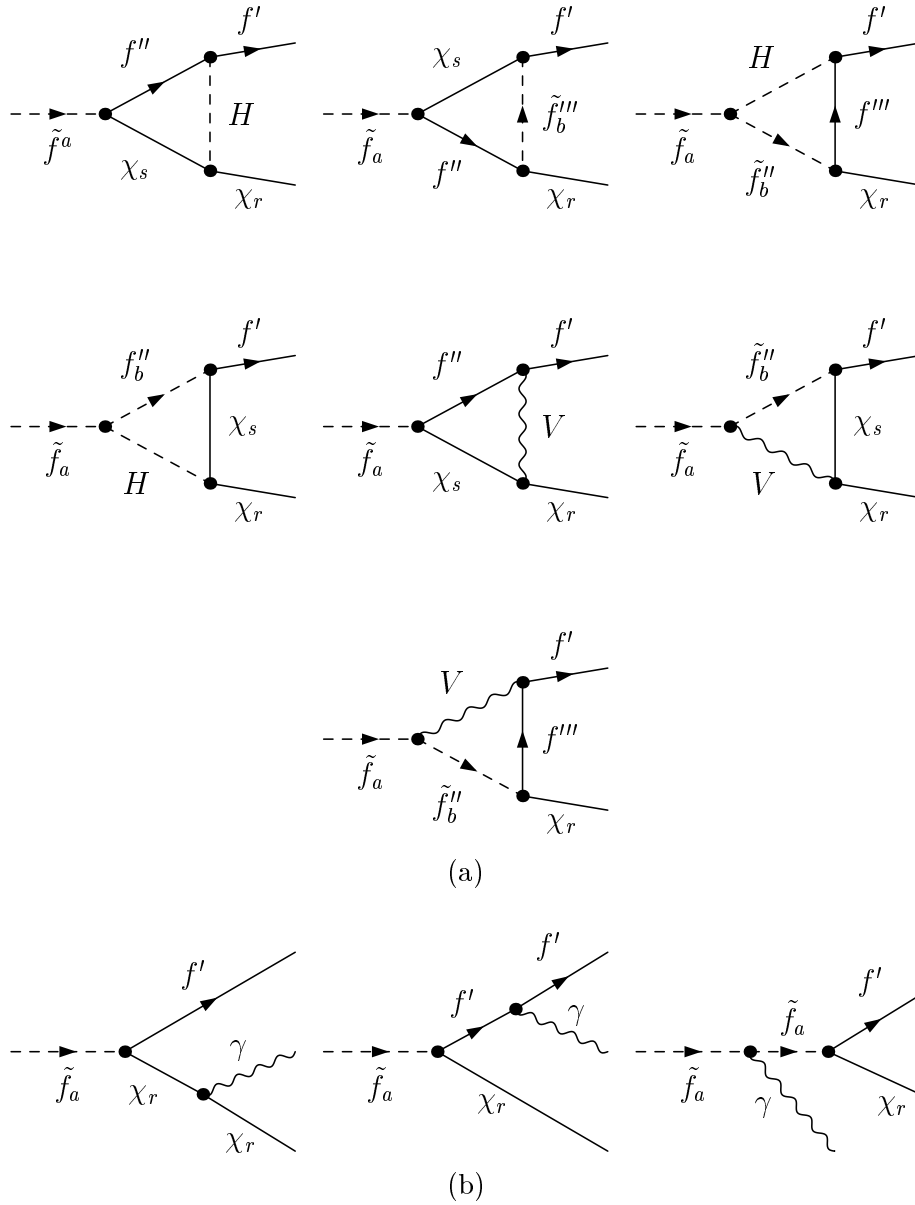


Figure 2: Feynman diagrams contributing to **a)** one-loop one-particle-irreducible three-point vertex functions Λ^{1PI} – eq. (41); **b)** tree-level photon bremsstrahlung. Notation as in Fig. 1.

We are now ready to compute the partial decay widths. The tree-level expressions read

$$\begin{aligned} \Gamma_{ar}^0 &= \Gamma^0(\tilde{f}_a \rightarrow f' \chi_r) = \frac{g^2}{16 \pi m_{\tilde{f}_a}^3} \lambda(m_{\tilde{f}_a}^2, M_r^2, m_{f'}^2) \times \\ &\times \left[(m_{\tilde{f}_a}^2 - M_r^2 - m_{f'}^2) (|A_{+ar}^{(f)}|^2 + |A_{-ar}^{(f)}|^2) - 4 m_{f'} M_r \text{Re} \left(A_{+ar}^{(f)} A_{-ar}^{(f)*} \right) \right], \end{aligned} \quad (43)$$

with $\lambda(x^2, y^2, z^2) = \sqrt{[x^2 - (y - z)^2][x^2 - (y + z)^2]}$.

Due to the presence of photon loops, the one-loop partial decay width computed using the amplitude (41) is infrared divergent; hence, bremsstrahlung of real photons has to be added to cancel this divergence. We therefore include in our results the radiative partial decay width $\Gamma(\tilde{f}_a \rightarrow f' \chi_r \gamma)$, including both the soft and the hard photon part.¹⁴ The corresponding Feynman diagrams are shown in Fig. 2b. This yields finally the complete one-loop electroweak correction,

$$\begin{aligned} \delta^{ar} &= \frac{\Gamma(\tilde{f}_a \rightarrow f' \chi_r)}{\Gamma^0(\tilde{f}_a \rightarrow f' \chi_r)} - 1 = \delta_{\text{virt}}^{ar} + \frac{\Gamma(\tilde{f}_a \rightarrow f' \chi_r \gamma)}{\Gamma^0(\tilde{f}_a \rightarrow f' \chi_r)}, \\ \delta_{\text{virt}}^{ar} &= 2 \text{Re} \left[(m_{\tilde{f}_a}^2 - M_r^2 - m_{f'}^2) (A_{+ar}^{(f)} C_{+ar}^{(f)} + A_{-ar}^{(f)} C_{-ar}^{(f)}) \right. \\ &\quad \left. - 2 M_r m_{f'} (A_{+ar}^{(f)} C_{-ar}^{(f)} + A_{-ar}^{(f)} C_{+ar}^{(f)}) \right] \times \\ &\quad \left[(m_{\tilde{f}_a}^2 - M_r^2 - m_{f'}^2) (|A_{+ar}^{(f)}|^2 + |A_{-ar}^{(f)}|^2) - 4 M_r m_{f'} \text{Re} (A_{+ar}^{(f)} A_{-ar}^{(f)*}) \right]^{-1}. \end{aligned} \quad (44)$$

The loop computation itself is rather tedious, since there is a huge number of diagrams to compute. This is better done by means of automatized tools. The computation of the loop diagrams has been performed by using the Computer Algebra Systems *FeynArts 3* and *FormCalc 2.2* [37, 38]. We have produced a set of Computer Algebra programs that compute the one-loop diagrams (and the bremsstrahlung corrections), which are then plugged into a *Fortran* code for the numerical evaluation with the help of the one-loop routines *LoopTools 1.2* [38]. A number of checks have been made on the results. The UV and infra-red finiteness of the result, relying on the relations between the different sectors of the model, is a non-trivial check. We also have recovered results already available in the literature; for instance, we used our set of programs to reproduce the strong corrections of [11], and, using the *higgsino* approximation, we could also reproduce the results of [21]. Moreover we also checked that, when using the $\overline{\text{MS}}$ -scheme, the one-loop corrections to neutralino and chargino masses reproduce those of [31].

Although we consider the chargino and neutralino masses as input parameters, in our numerical study we treat them in a slightly different way. We choose a set of renormalized input parameters (M, M', μ) , and apply (20), (22) to obtain the one-loop renormalized masses. Of course, if SUSY would be discovered the procedure will be the other way around, that is, the MSSM parameters will be computed from the various observables measured, for example, from the chargino production cross-section and asymmetries at the LC [33]. For a consistent treatment, the one-loop expressions for these observables will have to be used [39].

¹⁴Except for the partial decay width $\Gamma(\tilde{\nu} \rightarrow \nu \chi_\alpha^0 \gamma)$, which is obviously zero at tree-level.

2.5 Universal corrections: Non-decoupling effects and effective coupling matrices

We note that there exists a certain combination of contributions in the one-loop amplitude (41) that does not depend on the sfermion flavour. These contributions can be expressed formally as corrections to the coupling matrices

$$\tilde{U} = U + \Delta U \quad , \quad \tilde{V} = V + \Delta V \quad , \quad \tilde{N} = N + \Delta N \quad , \quad (45)$$

with

$$\begin{aligned} \Delta U_{i1} &\equiv U_{i1} \left(\frac{\delta g}{g} + \frac{\delta Z_R^{-i}}{2} \right) + U_{j1} \mathcal{Z}_R^{-ji} \quad , \\ \Delta U_{i2} &\equiv U_{i2} \left(\frac{\delta g}{g} + \frac{\delta Z_R^{-i}}{2} - \frac{1}{2} \frac{\delta M_W^2}{M_W^2} - \frac{\delta \cos \beta}{\cos \beta} \right) + U_{j2} \mathcal{Z}_R^{-ji} \quad , \\ \Delta V_{i1} &\equiv V_{i1} \left(\frac{\delta g}{g} + \frac{\delta Z_L^{-i}}{2} \right) + V_{j1} \mathcal{Z}_L^{-ji} \quad , \\ \Delta V_{i2} &\equiv V_{i2} \left(\frac{\delta g}{g} + \frac{\delta Z_L^{-i}}{2} - \frac{1}{2} \frac{\delta M_W^2}{M_W^2} - \frac{\delta \sin \beta}{\sin \beta} \right) + V_{j2} \mathcal{Z}_L^{-ji} \quad , \\ \Delta N_{\alpha 1} &\equiv N_{\alpha 1} \left(\frac{\delta g}{g} + \frac{\delta Z_R^{0\alpha}}{2} + \frac{\delta t_W}{t_W} \right) + \sum_{\beta \neq \alpha} N_{\beta 1} \mathcal{Z}_R^{0\beta\alpha} \quad , \\ \Delta N_{\alpha 2} &\equiv N_{\alpha 2} \left(\frac{\delta g}{g} + \frac{\delta Z_R^{0\alpha}}{2} \right) + \sum_{\beta \neq \alpha} N_{\beta 2} \mathcal{Z}_R^{0\beta\alpha} \quad , \\ \Delta N_{\alpha 3} &\equiv N_{\alpha 3} \left(\frac{\delta g}{g} + \frac{\delta Z_R^{0\alpha}}{2} - \frac{1}{2} \frac{\delta M_W^2}{M_W^2} - \frac{\delta \cos \beta}{\cos \beta} \right) + \sum_{\beta \neq \alpha} N_{\beta 3} \mathcal{Z}_R^{0\beta\alpha} \quad , \\ \Delta N_{\alpha 4} &\equiv N_{\alpha 4} \left(\frac{\delta g}{g} + \frac{\delta Z_R^{0\alpha}}{2} - \frac{1}{2} \frac{\delta M_W^2}{M_W^2} - \frac{\delta \sin \beta}{\sin \beta} \right) + \sum_{\beta \neq \alpha} N_{\beta 4} \mathcal{Z}_R^{0\beta\alpha} \quad , \\ \frac{\delta g}{g} &\equiv \frac{1}{2} \left(\frac{\delta \alpha}{\alpha} + \frac{c_W^2}{s_W^2} \left(\frac{\delta M_W^2}{M_W^2} - \frac{\delta M_Z^2}{M_Z^2} \right) \right) \quad . \end{aligned} \quad (46)$$

Unfortunately the full contributions to the expressions (46) are divergent. The only consistent subset of corrections which makes all the expressions in (46) finite is the subset of fermion and sfermion loops contributing to the self-energies of the gauge bosons, Higgs bosons, charginos and neutralinos. With this restriction, we can define *effective coupling matrices*

$$U^{eff} = U + \Delta U^{(f)} \quad , \quad V^{eff} = V + \Delta V^{(f)} \quad , \quad N^{eff} = N + \Delta N^{(f)} \quad , \quad (47)$$

where $\Delta U^{(f)}$, $\Delta V^{(f)}$, $\Delta N^{(f)}$ are given by the expressions (46) taking into account only loops of fermions and sfermions. We will refer to these corrections as *universal corrections*. They are the equivalent of the *super-oblique corrections* of Ref. [12].

These effective coupling matrices present a very interesting feature. Since the divergences in the SM sector of the model (gauge and Higgs sectors) cancel the divergences of the chargino-neutralino sector, the associated logarithmic terms ($\log(m/\mu^D)$, μ^D being the arbitrary mass parameter of dimensional reduced integrals) must be combined. As a result, a non-decoupling term $\sim \log(m^{SUSY}/m^{SM})$ appears in the final expression. Here m^{SUSY} represents a generic SUSY mass, and m^{SM} a generic SM mass.

We have checked explicitly this effect. We have computed analytically the electron-selectron contributions to the ΔU and ΔV matrices (46), assuming zero mixing angle in the selectron sector ($\theta_e = 0$), we have identified the leading terms in the approximation $m_{\tilde{e}_i}, m_{\tilde{\nu}} \gg (M_W, M_i) \gg m_e$, and analytically canceled the divergences and the $\log(\mu^D)$ terms; finally, we have kept only the terms logarithmic in the slepton masses. The result reads as follows:

$$\begin{aligned}
\Delta U_{i1}^{(f)} &= \frac{\alpha}{4\pi s_W^2} \log\left(\frac{M_{\tilde{e}_L}^2}{M_X^2}\right) \left[\frac{U_{i1}^3}{6} - U_{i2} \frac{\sqrt{2} M_W (M c_\beta + \mu s_\beta)}{3(M^2 - \mu^2)(M_1^2 - M_2^2)^2} (M^4 - M^2 \mu^2 + \right. \\
&\quad \left. + 3M^2 M_W^2 + \mu^2 M_W^2 + M_W^4 + M_W^4 c_{4\beta} + (\mu^2 - M^2) M_i^2 + 4M\mu M_W^2 s_{2\beta}) \right], \\
\Delta U_{i2}^{(f)} &= \frac{\alpha}{4\pi s_W^2} \log\left(\frac{M_{\tilde{e}_L}^2}{M_X^2}\right) U_{i1} \frac{M_W (M c_\beta + \mu s_\beta)}{3\sqrt{2}(M^2 - \mu^2)(M_1^2 - M_2^2)^2} \times \\
&\quad \times \left((M^2 - \mu^2)^2 + 4M^2 M_W^2 + 4\mu^2 M_W^2 + 2M_W^4 + 2M_W^4 c_{4\beta} + 8M\mu M_W^2 s_{2\beta} \right), \\
\Delta V_{i1}^{(f)} &= \frac{\alpha}{4\pi s_W^2} \log\left(\frac{M_{\tilde{e}_L}^2}{M_X^2}\right) \left[\frac{V_{i1}^3}{6} - V_{i2} \frac{\sqrt{2} M_W (\mu c_\beta + M s_\beta)}{3(M^2 - \mu^2)(M_1^2 - M_2^2)^2} (M^4 - M^2 \mu^2 + \right. \\
&\quad \left. + 3M^2 M_W^2 + \mu^2 M_W^2 + M_W^4 + M_W^4 c_{4\beta} + (\mu^2 - M^2) M_i^2 + 4M\mu M_W^2 s_{2\beta}) \right], \\
\Delta V_{i2}^{(f)} &= \frac{\alpha}{4\pi s_W^2} \log\left(\frac{M_{\tilde{e}_L}^2}{M_X^2}\right) V_{i1} \frac{M_W (\mu c_\beta + M s_\beta)}{3\sqrt{2}(M^2 - \mu^2)(M_1^2 - M_2^2)^2} \times \\
&\quad \times \left((M^2 - \mu^2)^2 + 4M^2 M_W^2 + 4\mu^2 M_W^2 + 2M_W^4 + 2M_W^4 c_{4\beta} + 8M\mu M_W^2 s_{2\beta} \right),
\end{aligned} \tag{48}$$

$M_{\tilde{e}_L}^2$ being the soft-SUSY-breaking mass of the $(\tilde{e}_L, \tilde{\nu})$ doublet (3), whereas M_X is a SM mass. In the on-shell scheme for the SM electroweak theory we define parameters at very different scales, basically $M_X = M_W$ and $M_X = m_e$. These wide-ranging scales enter the structure of the counterterms – see the last formula in eq.(46)– and so must appear in eq.(48) too. As a result the leading log in the various terms of this equation will vary accordingly. For simplicity in the notation we have factorized $\log M_{\tilde{e}_L}^2/M_X^2$ as an overall factor. In some cases this factor can be very big, $\log M_{\tilde{e}_L}^2/m_e^2$; it comes from the electron-selectron contribution to the chargino-neutralino self-energies. Its non-decoupling behaviour is logarithmic in the heavy (SUSY) mass and it can be explained from renormalization group arguments relating the supersymmetric gauge couplings at the SM and SUSY scales (see below). This term is similar to the logarithmic part of the universal effects from the SM gauge bosons, which is related to the renormalization of the ordinary

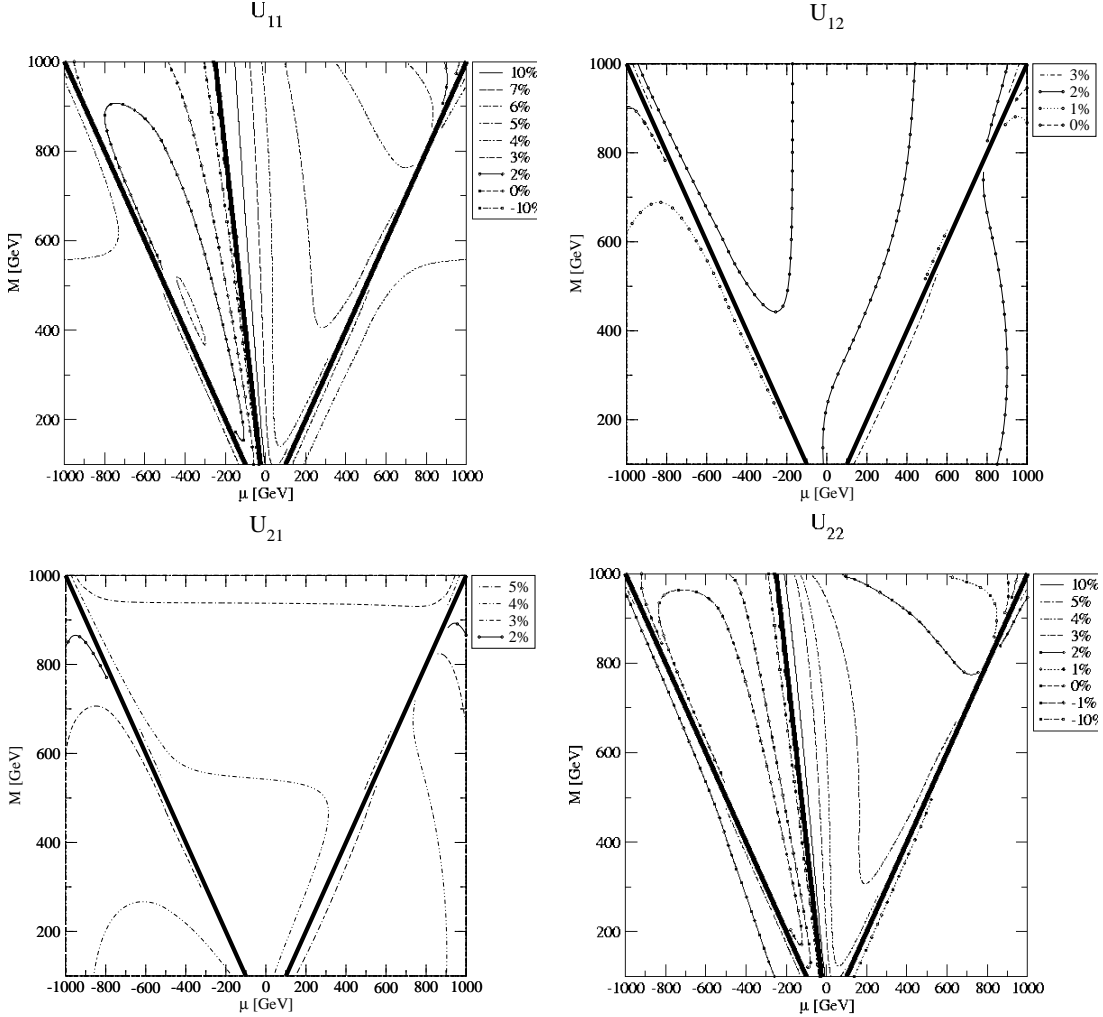


Figure 3: Correction to the effective chargino coupling matrix $\Delta U^{(f)}$ –eq. (46)– in the $M - \mu$ plane, for $\tan \beta = 4$ and a sfermion spectrum around 1 TeV (49).

gauge couplings and of course can also be explained by renormalization group arguments – in this case involving the internal SM scales M_W and m_e . Equivalent expressions can be found for the quark-squark sector. We have checked numerically that the expressions (48) approximate well the logarithmic term in the full expression (47). We have computed numerically (47) for different input parameters (including $\theta_e \neq 0$) for selectron masses in the range $m_{\tilde{e}_1} = 1 - 100$ TeV, we have fitted this numerical results to a simple function $f(m_{\tilde{e}_1}) = A + B \log(m_{\tilde{e}_1})$. The results show a correlation factor close to ± 1 in better than 10^{-4} . The simple expressions (48) approximate the coefficient of the logarithmic term in better than 1%.

However, the expressions (48) do not reproduce the full result (47) due to the presence of important non-logarithmic terms. Upon adding up the three slepton generations, the contributions to (47) can be typically of the order of $\sim 3\%$ for $m_{\tilde{e}_1} = 1$ TeV, whereas the

approximation (48) gives $\sim 2\%$ under the same conditions.

We want to stress that this is a physical, measurable, effect. By measuring the two chargino masses (M_1, M_2), one can extract the SUSY parameters M and $|\mu|$, and by assuming CP-conservation one can obtain the renormalized mixing matrices U and V for each sign of μ . On the other hand, one can extract the value of the mixing matrices in a polarized e^+e^- linear collider [33]. However, the extracted values of the mixing matrices are, in a first approximation, the ones of eq. (47), which can deviate from the on-shell ones –eq. (22)– at the several percent level. In this way, even if some (or all) of the sfermions have masses beyond the reach of an e^+e^- linear collider, one can get information of their mass scale by means of the effective coupling matrices. In fact, the larger the mass, the larger is the correction. Of course, the experimental value of the cross-section $\sigma(e^+e^- \rightarrow \chi^+\chi^-)$ will have to be compared with the full one-loop computed cross-section [39], since the rest of the one-loop corrections can be as large the contribution of the effective coupling matrices (47).

The ultimate reason for these non-decoupling effects lies in the breaking of SUSY, which affects the SUSY relation between the gauge-boson and gaugino couplings (or Higgs-boson and higgsino couplings). As a simple example, SUSY implies that the $e^+e^- \gamma$ coupling must be equal to the $\tilde{e}^+e^- \tilde{\gamma}$ coupling. For broken SUSY, this equality is lost, and the deviation of the $\tilde{e}^+e^- \tilde{\gamma}$ -coupling from the $e^+e^- \gamma$ -coupling grows with the scale of the SUSY breaking [12, 10]. One can understand the appearance of the non-decoupling effects by renormalization group arguments. In an energy scale much larger than any SUSY mass scale ($Q \gg m^{SUSY}$) the theory is supersymmetric, and the effective $e^+e^- \gamma$ gauge coupling ($\alpha(Q)$) is equal to the effective $\tilde{e}^+e^- \tilde{\gamma}$ Yukawa coupling ($\tilde{\alpha}(Q)$), and their renormalization group equations (RGE) are the same. If some hierarchy exists in the SUSY sector (say, for definiteness $m_{\tilde{q}} > m_{\tilde{e}}$), at the scale $Q = m_{\tilde{q}}$ the squarks decouple from the running of α and $\tilde{\alpha}$. Quarks, on the other hand, decouple from $\tilde{\alpha}$ but not from α . Therefore, at scales $Q < m_{\tilde{q}}$, the coupling $\tilde{\alpha}$ is frozen at the squark mass scale $\tilde{\alpha}(Q < m_{\tilde{q}}) = \tilde{\alpha}(m_{\tilde{q}}) = \alpha(m_{\tilde{q}})$ as far as quark/squark contributions are concerned¹⁵. Therefore, the comparison between the two couplings gives, at one-loop order:

$$\frac{\tilde{\alpha}(Q)}{\alpha(Q)} - 1 = \frac{\alpha(m_{\tilde{q}})}{\alpha(Q)} - 1 = \beta \log \frac{m_{\tilde{q}}}{Q} \quad , \quad Q < m_{\tilde{q}} \quad ,$$

where the QED β -function does not include the contribution from squarks. Since we are using an on-shell renormalization scheme, we are comparing in fact $\tilde{\alpha}(Q)/\alpha(0)$, and since the quarks decouple from α at $Q = m_q$, we end up with a correction proportional to $\log m_{\tilde{q}}/m_q$. We have explicitly checked this fact using SUSY Quantum Electrodynamics as a toy model. The complete electroweak model looks much cumbersome, since various quantities are fixed at different scales (e.g. the masses of the gauge bosons M_W, M_Z are fixed at their respective pole values, and the electromagnetic constant is fixed in the Compton limit $\alpha(0)$), therefore different pieces of the corrections carry different scales Q in the arguments of the logarithms.

¹⁵Of course, there is an evolution of $\tilde{\alpha}(Q < m_{\tilde{q}})$ due to the lepton/slepton contributions. Here we leave the slepton contributions out of the discussion for the sake of clarity.

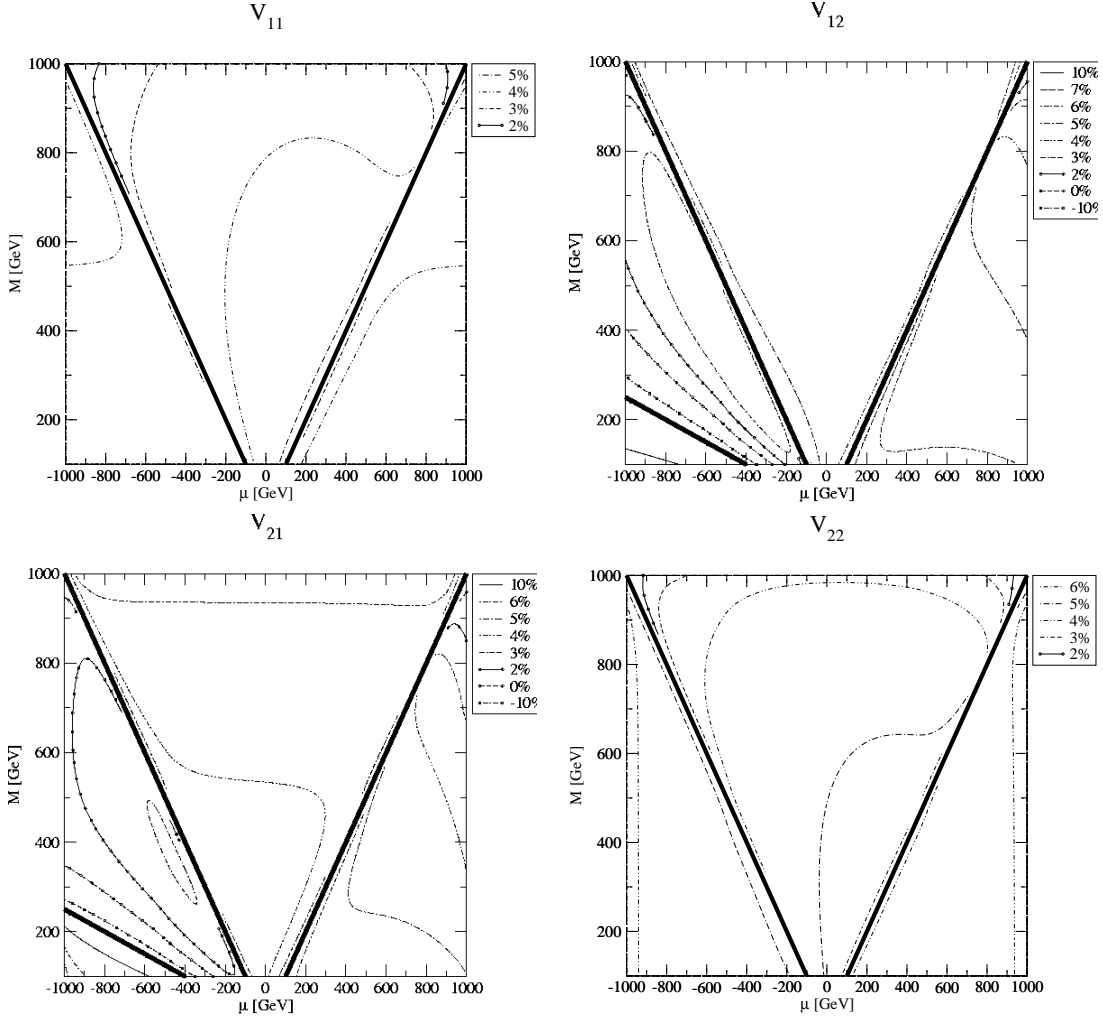


Figure 4: As in Fig. 3 but for the effective chargino coupling matrix $\Delta V^{(f)}$ –eq. (46).

In Figs. 3 and 4 we show contour plots in the $M - \mu$ plane of the relative correction to the elements of the mixing matrices U and V (47). For this figure we have chosen a sfermion spectrum around 1 TeV, namely:

$$\begin{aligned} \tan \beta = 4, \quad m_{\tilde{l}_2} = m_{\tilde{d}_2} = m_{\tilde{u}_2} = 1 \text{ TeV}, \quad m_{\tilde{l}_1} = m_{\tilde{d}_1} = m_{\tilde{l}_2} + 5 \text{ GeV}, \\ \theta_l = \theta_q = \theta_b = 0, \quad \theta_t = -\pi/5, \end{aligned} \quad (49)$$

where we have assumed a common mass for all the charged sleptons and down-type quarks, and considered mixing only in the stop sector.

The thick black lines in Figs. 3-4 correspond to spurious divergences in the relative corrections. The ones corresponding to $M = \pm\mu$ are divergences in the corrections themselves, since our renormalization prescription fails in this case –see eq. (29). This divergence appears also explicitly in the approximate expression (48) as the inverse of $M^2 - \mu^2$. The other divergences correspond to lines where the renormalized mixing matrix elements are

zero. These correspond to $M = -\mu \tan \beta$ ($M = -\mu / \tan \beta$) for U_{11}, U_{22} (V_{12}, V_{21}). Corrections as large as $\pm 10\%$ can only be found in the vicinity of these divergence lines. However, there exist large regions of the $\mu - M$ plane where the corrections are larger than 2%, 3%, or even 4%.

3 Numerical evaluation

In this section we tackle the (cumbersome) numerical analysis of the corrections to the various $\tilde{f} \rightarrow f' \chi$ partial decay channels according to the following plan. First of all we assess the relevance of the universal corrections defined in sect. 2.5. Next we focus on the non-universal corrections, with especial emphasis on the non-decoupling effects from gauginos and Higgs particles, followed by an exhaustive analysis of the corrections to the various partial decay widths as a function of the most relevant parameters. After that, we briefly concentrate on the strong corrections. Finally, we combine the universal, non-universal, and strong corrections to the partial decay widths to evaluate the impact on the branching ratios for all the decay channels, which are in practice the true observables.

As for the presentation of the results themselves, we will use the following criteria: The first and second generation of sfermions have very similar properties, so only the results for the first generation are presented. We will present separate results for the third squark generation (\tilde{t}, \tilde{b}), since the large Yukawa couplings and masses make this generation behave in a special way. The third generation sleptons ($\tilde{\tau}, \tilde{\nu}_\tau$) have also large Yukawa couplings, but their effect is small, unless $\tan \beta$ is very large. We will refrain to show explicit results for $\tilde{\tau}, \tilde{\nu}_\tau$, if these results are similar to the first generation ones.

We have used the following default set of central parameters for our numerical evaluation:

$$\begin{aligned}
m_t &= 175 \text{ GeV} , m_b = 5 \text{ GeV} , \tan \beta = 4 , M_{H^\pm} = 120 \text{ GeV} , \\
m_{\tilde{b}_2} &= m_{\tilde{d}_2} = m_{\tilde{u}_2} = m_{\tilde{e}_2} = 300 \text{ GeV} , \\
m_{\tilde{b}_1} &= m_{\tilde{d}_1} = m_{\tilde{e}_1} = m_{\tilde{b}_2} + 5 \text{ GeV} , m_{\tilde{u}_2} = 290 \text{ GeV} , m_{\tilde{t}_2} = 300 \text{ GeV} , \\
\theta_b &= \theta_d = \theta_u = \theta_e = 0 , \theta_t = -\pi/5 , \\
\mu &= 150 \text{ GeV} , M = 250 \text{ GeV} .
\end{aligned} \tag{50}$$

We point out that the amount of splitting chosen in the sbottom sector is not critical for the numerical results, and has nothing to do with preserving the vacuum condition (6) because we are assuming zero sbottom mixing angle in the first eq.(5). Furthermore, the negative sign for the stop mixing angle is related to the chosen sign for μ and the desired relation $\mu A_t < 0$ via the second eq.(5). The other SM parameters have been taken from Ref. [40]. For simplicity, we will be using the Grand Unification (GUT) relation between the electroweak soft-SUSY-breaking gaugino masses $M' = 5 M t_W^2/3$ unless stated otherwise. The computed values of the heaviest up-type sfermions are given in table 1. In table 2 we show the tree-level chargino and neutralino masses, as well as the tree-level branching ratios of sfermions decaying into charginos and neutralinos, and the one-loop corrections to the neutralino masses.

	\tilde{u}_1	\tilde{t}_1	$\tilde{\nu}$
$m^{tree}[\text{GeV}]$	296	364	296
$\Delta m^{EW}/m^{tree}$	+0.06%	+0.26%	-0.06%
$\Delta m^{QCD}/m^{tree}$	-0.19%	-3.24%	-

Table 1: Tree-level masses and one-loop corrections for the heaviest up-type sfermion, for the parameter set (50).

	χ_1^0	χ_2^0	χ_3^0	χ_4^0	χ_1^+	χ_2^+
$m_\chi[\text{GeV}]$	86	149	156	290	119	289
$\Delta m_\chi/m_\chi$	-	1.89%	-0.56%	-0.09%	-	-
$BR(\tilde{\nu} \rightarrow l\chi)$	0.430	-	0.016	0.001	0.549	0.003
$BR(\tilde{e}_1 \rightarrow l\chi)$	0.018	0.610	0.004	0.010	0.328	0.030
$BR(\tilde{e}_2 \rightarrow l\chi)$	0.572	0.423	0.005	-	-	-
$BR(\tilde{\tau}_1 \rightarrow l\chi)$	0.021	0.606	0.007	0.010	0.325	0.030
$BR(\tilde{\tau}_2 \rightarrow l\chi)$	0.567	0.419	0.008	-	0.006	-
$BR(\tilde{u}_1 \rightarrow q\chi)$	0.026	0.257	0.007	0.002	0.704	0.004
$BR(\tilde{u}_2 \rightarrow q\chi)$	0.580	0.415	0.005	-	-	-
$BR(\tilde{d}_1 \rightarrow q\chi)$	0.317	0.107	0.021	0.019	0.491	0.045
$BR(\tilde{d}_2 \rightarrow q\chi)$	0.572	0.423	0.005	-	-	-
$BR(\tilde{t}_1 \rightarrow q\chi)$	0.169	0.249	0.145	-	0.159	0.278
$BR(\tilde{t}_2 \rightarrow q\chi)$	0.058	-	-	-	0.942	-
$BR(\tilde{b}_1 \rightarrow q\chi)$	0.272	0.092	0.047	0.014	0.575	-
$BR(\tilde{b}_2 \rightarrow q\chi)$	0.502	0.332	0.123	-	0.042	-

Table 2: Neutralino and chargino masses (and one-loop corrections), and tree-level branching ratios of sfermions into charginos and neutralinos for the parameter set (50). Branching ratios below 10^{-3} are not shown.

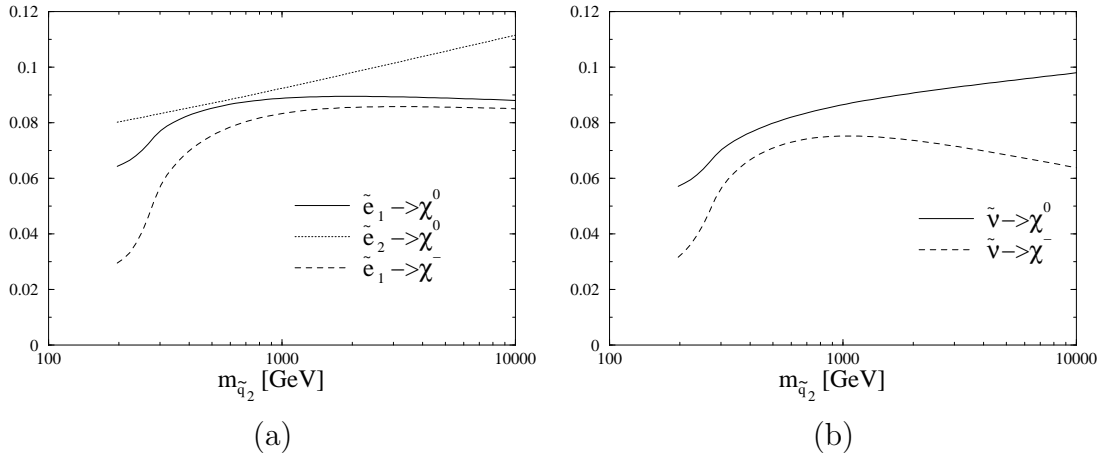


Figure 5: Universal corrections $\delta(\tilde{l}_a \rightarrow l' \chi)$ – see eq.(51) – to the partial decay widths of the first two generation of sleptons ($\tilde{l} = \tilde{e}, \tilde{\nu}_e$) as a function of a common squark mass.

Given the large number of decay channels, a presentation including the corrections to each individual final state would be tedious. Moreover, a large number of channels have a very small branching ratio, and higher-order terms are not of phenomenological interest. For these reasons most of the discussion will be devoted to the total decay widths of sfermions into charginos and neutralinos, in particular to the relative correction

$$\delta(\tilde{f}_a \rightarrow f' \chi) = \frac{\sum_r (\Gamma(\tilde{f}_a \rightarrow f' \chi_r) - \Gamma^0(\tilde{f}_a \rightarrow f' \chi_r))}{\sum_r \Gamma^0(\tilde{f}_a \rightarrow f' \chi_r)}, \quad (51)$$

with $\chi = \chi^\pm$ or $\chi = \chi^0$. We will not show results for processes whose branching ratio are less than 10% in all of the explored parameter space.

3.1 Universal Corrections

As we have said, we start our numerical analysis by testing the non-decoupling effects directly associated to the universal corrections discussed in section 2.5. The main aim of this section is to assess the numerical impact of these non-decoupling effects. To this end we present in Fig. 5 the universal corrections to the partial decay widths of the first generation of sleptons ($\tilde{e} - \tilde{\nu}_e$) as a function of a common mass for all squarks. Since these corrections are universal, and the lepton masses can be safely neglected, they are the same for the other generations of sleptons. Looking at the right end of the plots ($m_{\tilde{q}} > 10^3$ GeV), the logarithmic scale of the plots makes evident the non-decoupling of squarks by means of a logarithmic term $\log(m_{\tilde{q}})$ equivalent to that of eqs. (48). The corrections are also non-negligible for light squark masses. We see that for squark masses below 1 TeV the corrections reach a 5% value for most of the decay channels, or even larger than 10% for the selectron decay into neutralinos.

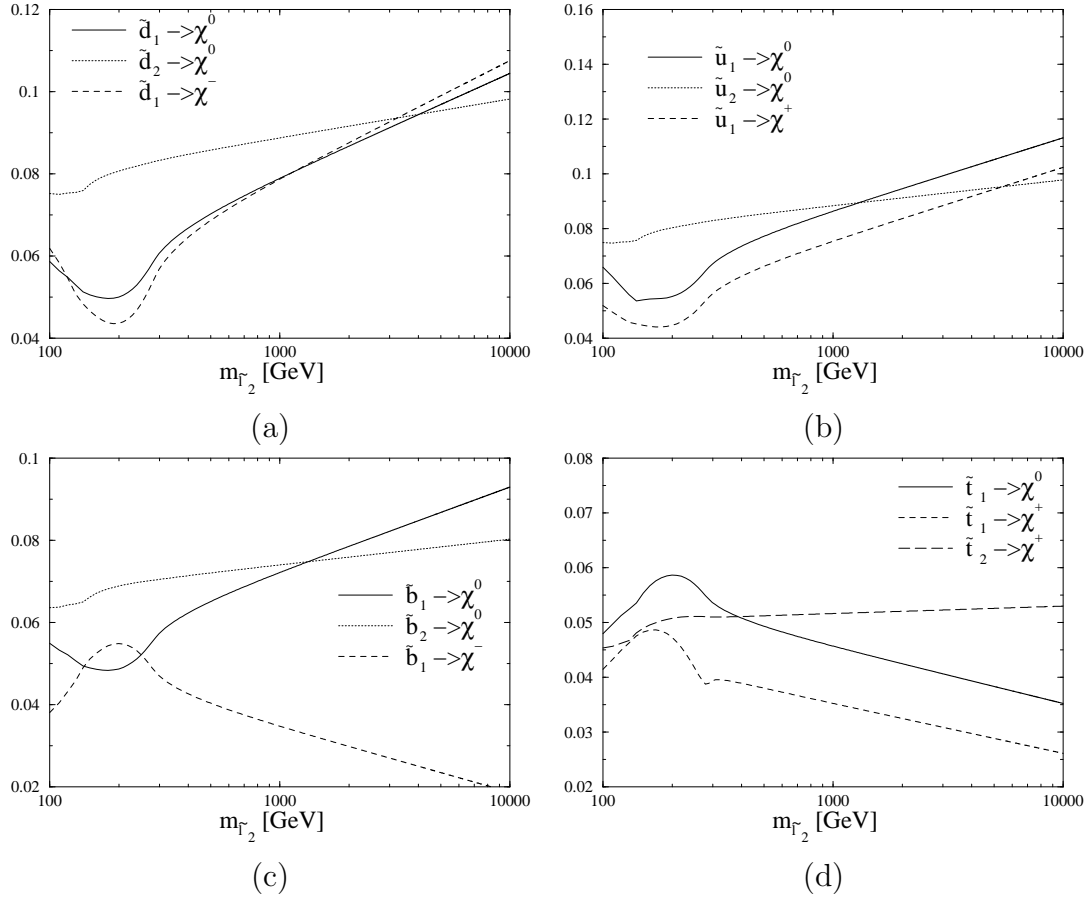


Figure 6: Universal corrections to the squark partial decay widths as a function of a common slepton mass, for the first and third generation of squarks.

We turn now our attention to the squark decays. Fig. 6 shows the universal corrections to the squark partial decay widths as a function of a common mass for all sleptons. We show the corrections for down-type and up-type quarks of the first and third generation. Again, the logarithmic behaviour from eq. (48) is evident in this figure. The logarithmic regime is attained already for slepton masses of order 1 TeV. The universal corrections are seen to be positive for all squark decays, ranging between 4% and 10% for slepton masses below 1 TeV.

3.2 Non-Universal corrections

The non-universal corrections comprise the set of full corrections excluding the universal corrections of section 2.5. For a given sfermion decay, these corrections do not depend on the parameters of the sfermions of different type or generation. That is, e.g. for a \tilde{t} decay, the dependence on the lepton/slepton parameters and the first and second generation quark/squark parameters appears only in the universal corrections analyzed in the previous section, and the non-universal corrections depend only on the gauge, Higgs, chargino/neutralino and stop/sbottom sectors.

3.2.1 Non-decoupling effects

The non-decoupling of gauginos was already discussed in [10, 11]. There, the QCD corrections to the squark decays were computed, and an explicit non-decoupling gaugino term (of the form $\log m_{\tilde{g}}$) was found. The origin of this non-decoupling effect is similar to that of the sfermionic ones in (48), namely the gaugino UV-divergences cancel the gauge boson ones, so that the logarithms associated with the divergence must compensate between SUSY and non-SUSY particles, leading to a $\log(M_{gaugino})$ behaviour which can again be explained from simple renormalization group arguments. The electroweak corrections present several peculiarities that prevent from obtaining a simple analytical result of these logarithms. First of all, the non-decoupling particles are part of the final state of the process, thus if their masses are large the decay will be phase-space closed. Second, the complicated structure of the electroweak sector involves the mixing of gauginos and higgsinos. One can not compute simply the gauge–gaugino or the Higgs–boson–higgsino corrections, unless very special limits are taken [21]. Thus, a numerical approach is preferred in this case.

In this subsection (3.2.1) we give up the GUT assumption between the gaugino masses, and will let the soft-SUSY-breaking mass parameters M and M' vary independently. In this way we can afford having a light neutralino (when M' is light), while the $SU(2)$ gauginos are heavy, and analyze the non-decoupling effects of the $SU(2)$ gauginos in the neutralino decays. On the other hand, by maintaining M light, but taking M' to be heavy, one obtains a heavy $U(1)_Y$ neutralino whose non-decoupling effects can be studied in the chargino sector.

In Fig. 7 we show the non-universal corrections to the slepton and squark decays into neutralinos as a function of the soft-SUSY-breaking $SU(2)$ gaugino mass parameter M in the range 1 – 10 TeV, keeping M' fixed to a light value $M' = 120$ GeV. For $M < 1$ TeV

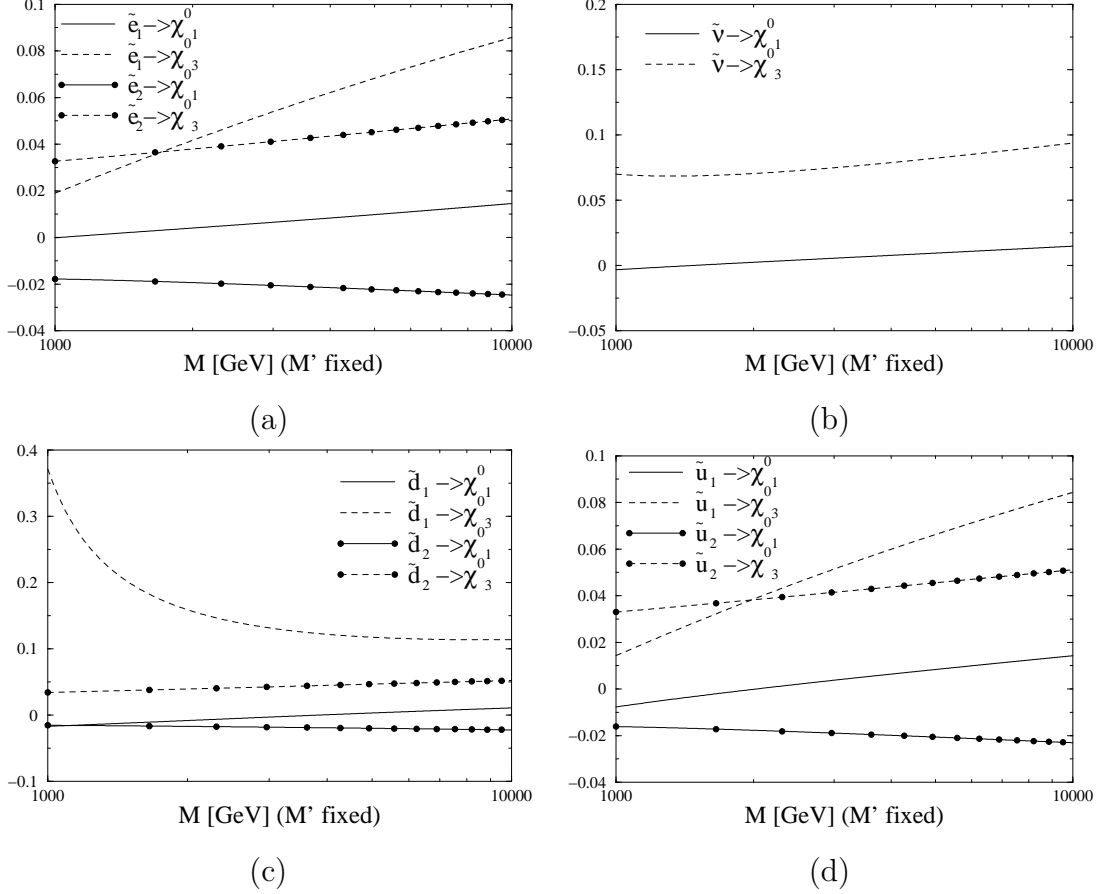


Figure 7: Non-universal corrections to the partial decay widths of first-generation sfermions into neutralinos, as a function of the soft-SUSY-breaking $SU(2)$ gaugino mass parameter M , keeping $M' = 120$ GeV. Shown are the corrections for each individual decay channel with a branching ratio larger than 10%.

the corrections show a rich structure that will be analyzed below. Only the results for the first generation of sfermions are shown; although the results for top- and bottom-squarks are slightly different, the same conclusion follows. Shown are the corrections for each individual decay channel with a branching ratio larger than 10%. For $M = 1$ TeV most of the decays have already reached the logarithmic regime, so the figure shows mainly straight lines. The corrections can have both signs, and range between 2% and 20% at $M = 1$ TeV. The slopes of the curves are small which means that, although there exist a non-decoupling effect, it is very small and of no phenomenological interest for $M < 10$ TeV.

A similar situation is found in the non-decoupling effect of the $U(1)_Y$ gaugino with respect to the decays into charginos in Fig. 8. In this case the slopes of the different curves are even smaller.

The non-decoupling effects from Higgs particles can be seen in Fig. 9. The figure makes

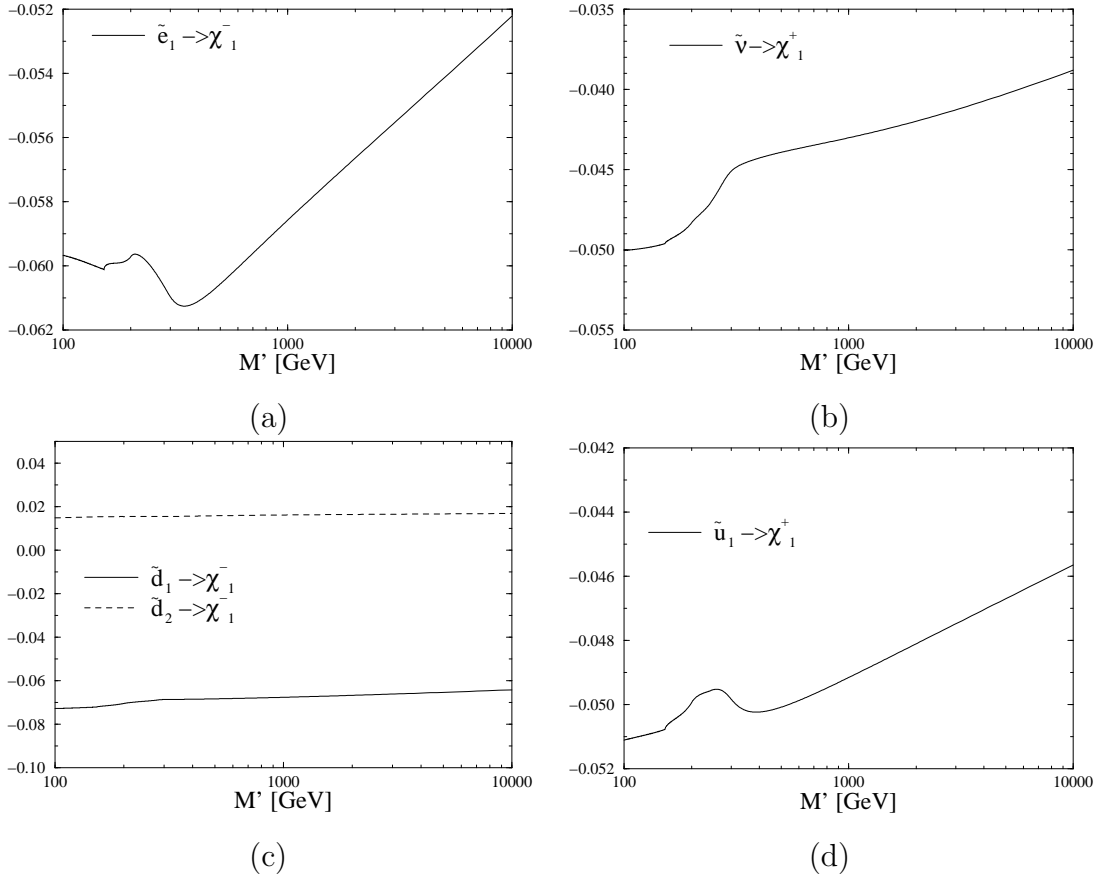


Figure 8: Non-universal corrections to the partial decay widths of first-generation sfermions into charginos, as a function of the soft-SUSY-breaking $U(1)_Y$ gaugino mass parameter M' , at fixed $M = 150$ GeV. Shown are the corrections for each individual decay channel with a branching ratio larger than 10%.

clear that the corrections grow as a $\log(M_{H^\pm})$. The effect is, of course, much larger in the third generation squark decays, but is also visible in the \tilde{e} and $\tilde{\nu}_e$ decays.

3.2.2 General analysis

We will present here the behaviour of the non-universal electroweak corrections as a function of parameters relevant for the chargino/neutralino sector and the sfermion sector, and $\tan\beta$. In general the corrections present a rich structure, due to the fact that every single parameter controls different aspects of the decay under study. Let's take for example the higgsino mass parameter μ . When changing this parameter, the neutralino and chargino masses change, and some decay channels open or close: when this happens, threshold divergences appear in the rest of the channels. At the same time, for $|\mu| = M$ our renormalization prescription breaks down (Cf. eq.(29)), and divergent corrections appear.

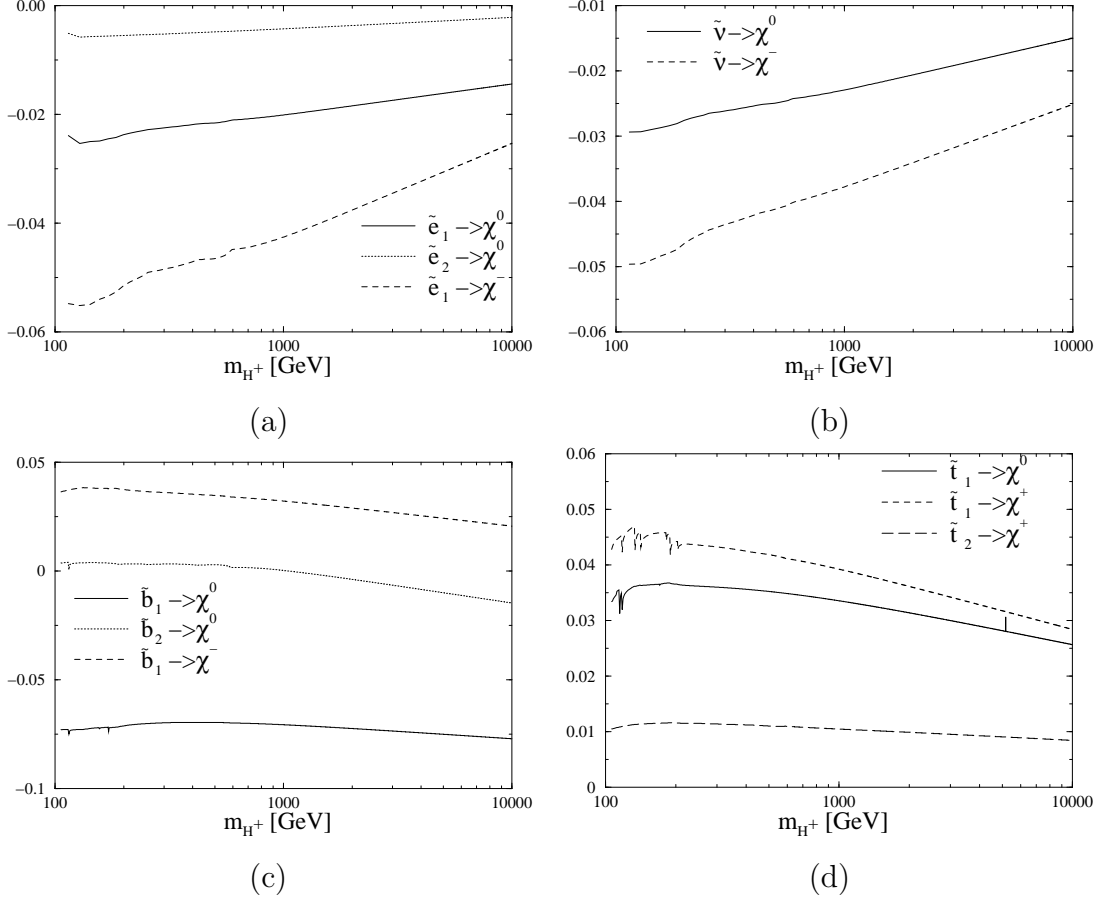


Figure 9: Non-universal corrections to the \tilde{e} , $\tilde{\nu}_e$, \tilde{b} and \tilde{t} partial decay widths, as a function of the charged Higgs mass. Shown are the corrections for each decay channel with a branching ratio larger than 10%.

Moreover the μ parameter enters the coupling of the sfermion to Higgs bosons in two ways: directly, in the expression of the Feynman rules, and indirectly, in the determination of the soft-SUSY-breaking trilinear couplings (5). As a result the variation of the corrections with respect to μ will exhibit a complicated evolution pattern spotted with the spurious divergences associated with the renormalization framework.

In Figs. 10 and 11 we display the corrections for the partial decay widths into neutralinos and charginos for sleptons and squarks respectively. In all plots we can see the divergences at $|\mu| = M$. We also see similar structures in several plots. These similarities make clear the $SU(2)$ structure of the theory, for example in the corrections to the partial decays of \tilde{e}_1 , $\tilde{\nu}_e$, $\tilde{\tau}_1$, \tilde{u}_1 and \tilde{d}_1 into charginos. The corresponding decays into neutralinos deviate among the different sfermions, since the $U(1)_Y$ charge enters the game. The presence of large Yukawa couplings also alters the general behaviour of the corrections. The corrections to the top- and bottom-squark decays exhibit indeed a very different structure. Differences in

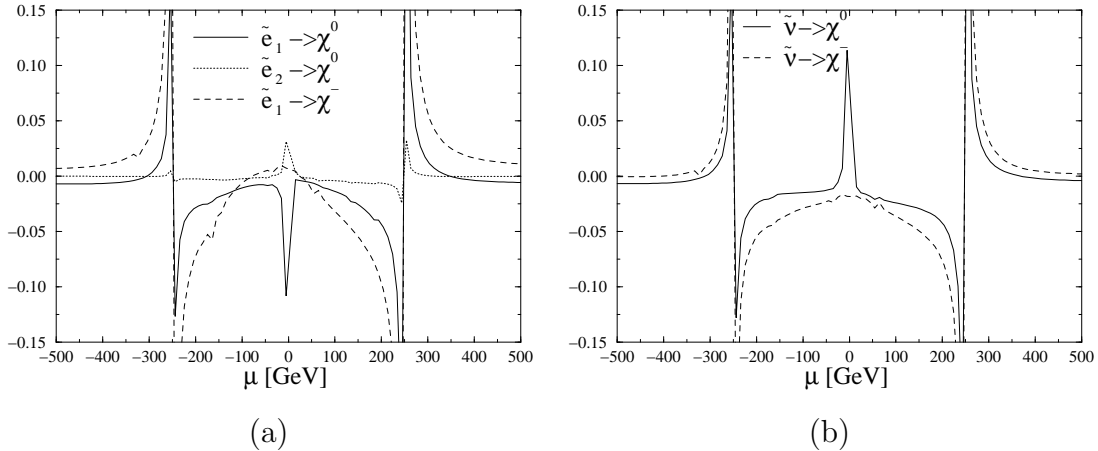


Figure 10: Non-universal corrections to the partial decay width of \tilde{e} and $\tilde{\nu}_e$ into charginos and neutralinos as a function of the higgsino mass parameter μ .

the $\tilde{\tau}$ decays would only be visible in the $\tilde{\tau}_2 \rightarrow \tilde{\nu}\chi^-$ decay channel, which has a branching ratio below 1% (see table 2).

Figs. 12 and 13 show the evolution with the soft-SUSY-breaking gaugino mass parameter M . Again we observe a very similar structure for the sleptons and the first generation squarks. For $M < |\mu|$, and away from the divergence region, the corrections are small (less than 5%) in most channels. Only the decay mode $\tilde{t}_2 \rightarrow b\chi^+$ has corrections around 10%. For $M > |\mu|$ the corrections can be moderate, up to 5% for the sleptons and first generation squarks, and 10% for the bottom-squarks. Note also the divergence appearing in the corrections to the \tilde{b} decays into χ^- when the value of the masses approach the phase space limit. This divergence arises from the Coulomb singularity due to soft-photon exchange between the two final state particles [41]. A consistent description of the decay width in this mass regime needs of a proper description of slowly moving final-state charged particles [42].

We now turn our view to the parameters of the sfermion sector. We start with the sfermion mixing angle. Its main effect is not in the corrections themselves, but in the tree-level decay amplitudes. In Fig. 14 we show the variation of the relative corrections as a function of relevant mixing angles. For the $\tilde{\tau}$ decays we see spikes of large corrections for the chargino channels. These spikes reflect the fact that near $\theta_\tau = 0$ ($\theta_\tau = \pm\pi/2$) the $\tilde{\tau}_2$ ($\tilde{\tau}_1$) has a tiny branching ratio to charginos; it is basically a $\tilde{\tau}_R$, which (at the tree-level) couples only to higgsino-type charginos with a small Yukawa coupling. At one-loop, however, the $\tilde{\tau}_R$ does effectively couple to charginos both through the one-loop conversion $\tilde{\tau}_R \rightarrow \tilde{\tau}_L$ and through genuine vertex diagrams. These contributions can be of the same size as the tree-level contributions, giving large corrections. For the sfermions of the first two generations these spikes are more pronounced. Since their Yukawa couplings are negligible, the one-loop effective coupling is larger than the tree-level one.

The third generation squarks have a very different behaviour. To understand Fig. 14b

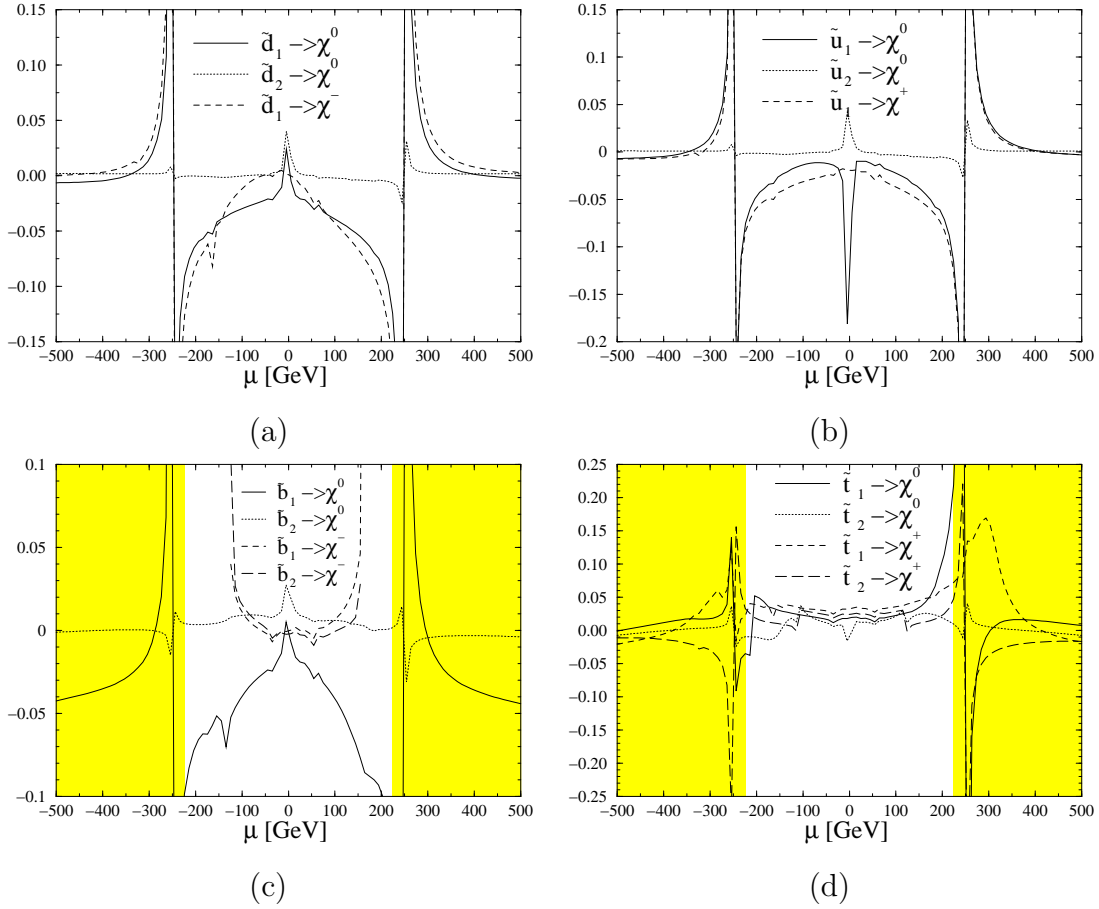


Figure 11: As in Fig. 10, but for the first and third generations of squarks. The shaded regions correspond to the violation of the condition (6).

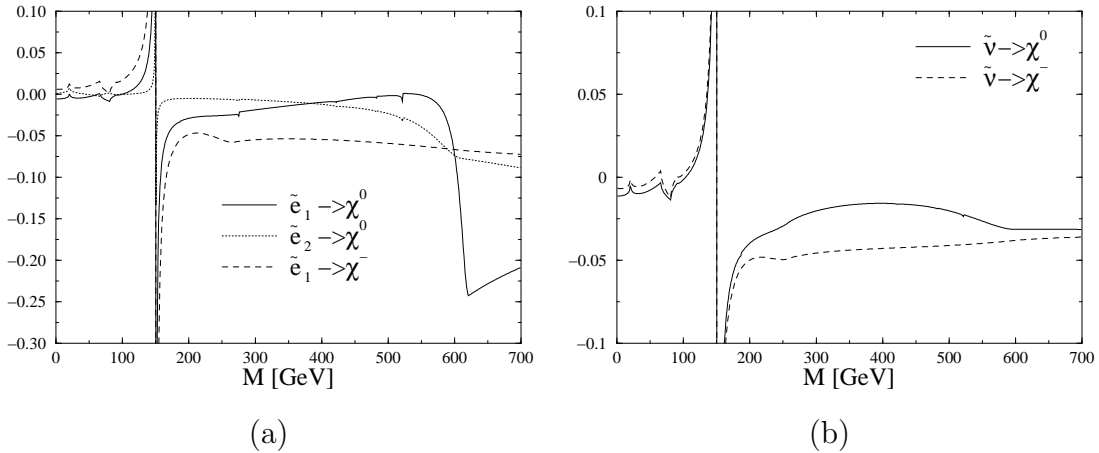


Figure 12: Non-universal corrections to the partial decay width of \tilde{e} and $\tilde{\nu}_e$ into charginos and neutralinos as a function of the gaugino mass parameter M .

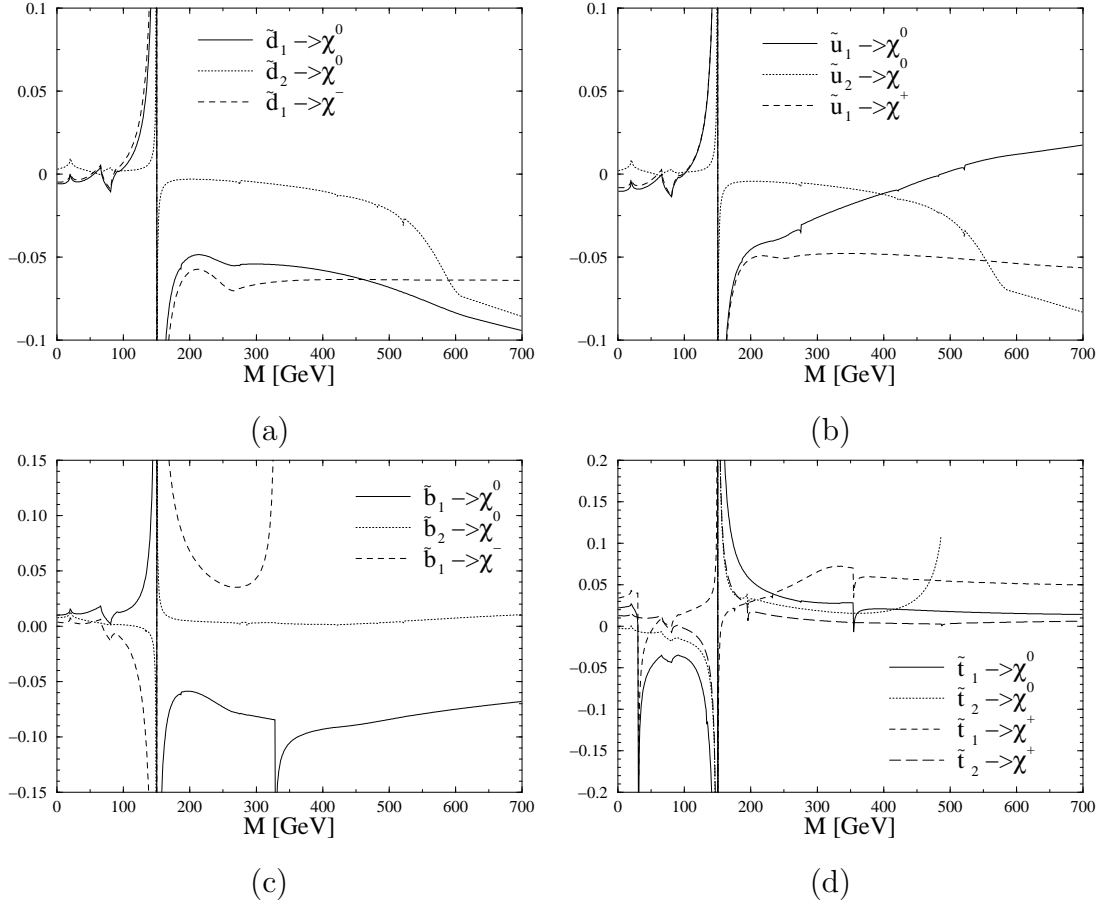


Figure 13: As in Fig. 12, but for the first and third generations of squarks.

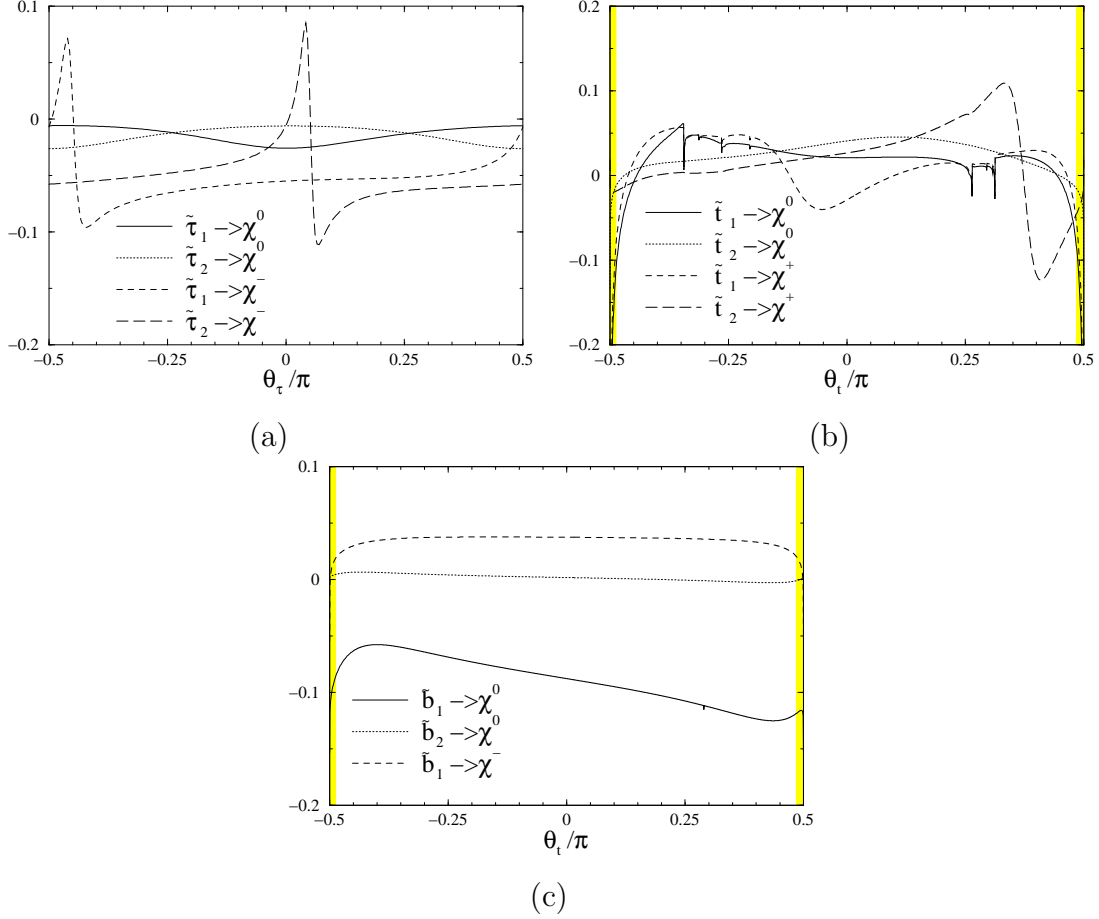


Figure 14: Non-universal corrections to the partial decay width of sfermions into charginos and neutralinos as a function of the sfermion mixing angles. **a)** $\tilde{\tau}$ decays as a function of the $\tilde{\tau}$ mixing angle $\theta_{\tilde{\tau}}$; **b)** \tilde{t} decays as a function of the \tilde{t} mixing angle $\theta_{\tilde{t}}$; and **c)** \tilde{b} decays as a function of the \tilde{t} mixing angle $\theta_{\tilde{t}}$. The shaded regions correspond to the violation of the condition (6).

one has to bear in mind that the heaviest squark mass varies with the squark mixing angle. As θ_t varies the \tilde{t}_1 mass crosses a series of thresholds. The corrections to the \tilde{t}_2 decays on the other hand have a smooth behaviour, similar to the $\tilde{\tau}$ decays but with the spikes softened by the larger Yukawa coupling.

We also show in Fig. 14c the variation of the bottom-squark decays as a function of the \tilde{t} mixing angle θ_t . Although the shape of the figure might be reminiscent of what would be obtained by the use of the finite threshold corrections to the bottom-quark Yukawa coupling [9, 43, 44], this is not the leading contribution to the corrections. In fact, we have checked that the use of the finite threshold corrections to the bottom-quark Yukawa coupling reproduce quite well the shape of the corrections to the \tilde{b}_2 ($\equiv \tilde{b}_R$) partial decay widths. However, there exist finite terms from other contributions, changing the overall value of the corrections. For the \tilde{b}_1 ($\equiv \tilde{b}_L$) the finite threshold corrections fail to give an approximate description of the full result.

The evolution with the sfermion mass parameters themselves can be seen in Figs. 15-16. In Fig. 15 we vary one of the sfermion masses, by maintaining the splitting between \tilde{f}_1, \tilde{f}_2 as in eq. (50). In Figs. 15a and b we show the non-universal corrections to the selectron and sneutrino partial decay widths. Above $m_{\tilde{f}} \gtrsim 1$ TeV the corrections follow the Sudakov double-log form $\delta \sim A + B \log^2(m_{\tilde{f}}^2/M_W^2)$ [45]. This kind of electroweak corrections appears in any observable in which the process energy is much larger than the electroweak mass scale. For comparison the universal contributions are shown in Figs. 15c and d as a function of a common slepton mass. While the universal effects dominate over the Sudakov terms in the relevant region where the sfermion masses lie below 1 TeV, the opposite holds once these masses become larger.

It is interesting to further explore the behaviour of the corrections in the mass region below 1 TeV also for the squark decays. In Fig. 16 we show the corrections for top- and bottom-squark decays as a function of the masses, in a mass range 100 – 600 GeV. In this figure the splitting between the bottom-squarks is fixed at 5 GeV, whereas the top-squark mass is left free. Several thresholds are seen in the figures. The value of the corrections behaves smoothly between the threshold points, but it is clear that the value of the corrections depends strongly on the exact correlation between the several MSSM masses.

We come finally to the $\tan \beta$ parameter. For the first two sfermion generations $\tan \beta$ only enters the corrections through the expressions of the masses, since the Yukawa couplings are negligible. As a consequence the evolution with $\tan \beta$ is flat above $\tan \beta \simeq 4$, when the masses acquire their asymptotic values.

For the third generation the couplings of fermions and sfermions with Higgs bosons and higgsinos loops enter the game. If we stick to the input parameters in (50) the trilinear soft-SUSY-breaking couplings A_f acquire large values – see eq. (5) – and the sfermion-Higgs couplings become large, and even non-perturbative. Note however, that large A_f values would generate charge and colour breaking vacuum – eq. (6). As long as the A_f are consistent with the (necessary) condition (6) the corrections remain perturbative. This is not to say that scenarios with $\tan \beta \gtrsim 5$ are not possible, but that, for a given $\tan \beta$, the

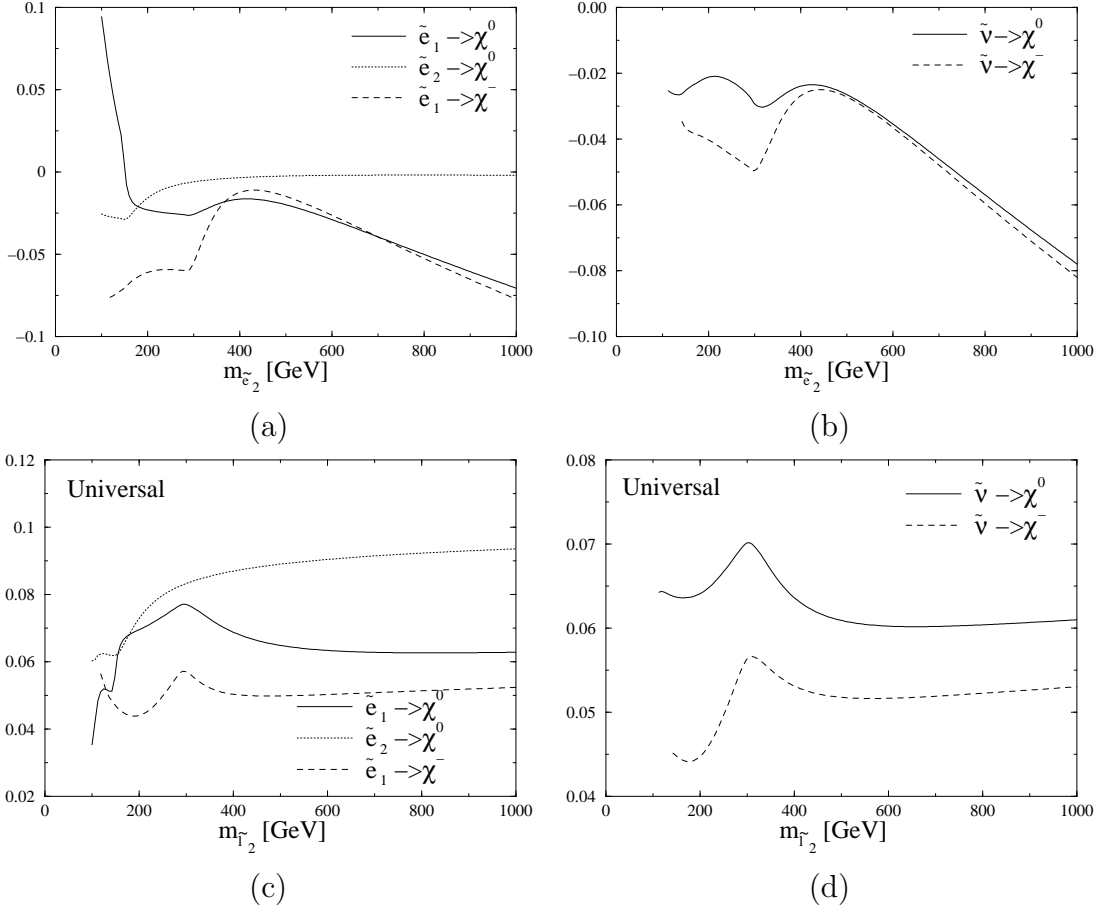


Figure 15: Corrections to the partial decay width of first generation sfermions into charginos and neutralinos. Non-universal contributions are shown in **a)** \tilde{e} and **b)** $\tilde{\nu}_e$ decays as a function of the lightest selectron mass $m_{\tilde{e}_2}$ maintaining $m_{\tilde{e}_1} = m_{\tilde{e}_2} + 5$ GeV. Also shown are the universal contributions to **a)** \tilde{e} and **b)** $\tilde{\nu}_e$ decays as a function of a common lightest slepton mass $m_{\tilde{l}_2}$ with $m_{\tilde{l}_1} = m_{\tilde{l}_2} + 5$ GeV.

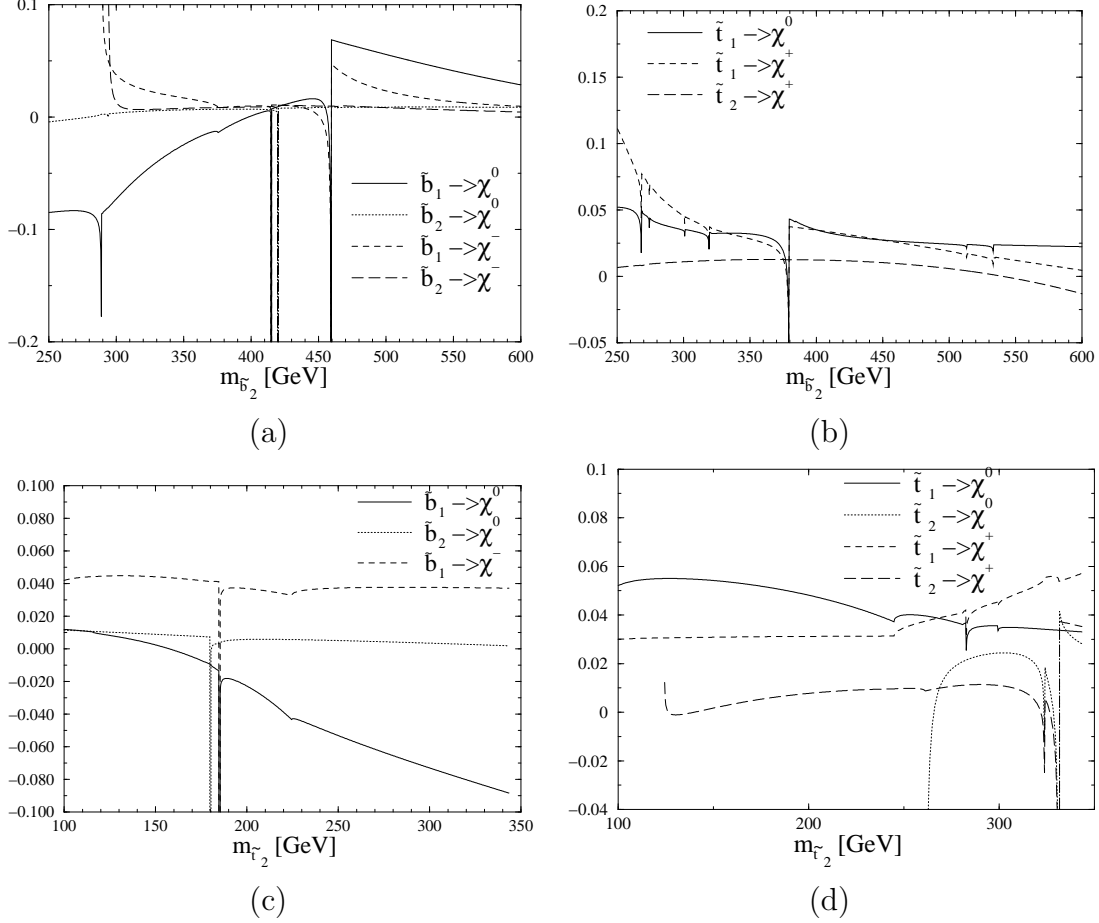


Figure 16: Non-universal corrections to the partial decay width of third generation squarks into charginos and neutralinos, as a function of **a)** and **b)** the lightest bottom-squark mass $m_{\tilde{b}_2}$; **c)** and **d)** the lightest top-squark mass $m_{\tilde{t}_2}$. The splitting between the sbottoms is as in eq.(50).

input parameters A_f , $m_{\tilde{f}_i}$ and θ_f are constrained so that eq. (6) is satisfied. In particular, note that a zero mixing angle in the sbottom sector is not possible for large $\tan\beta$. To probe the effect of $\tan\beta$ in the corrections we must choose a different parameter set that satisfies the bound (6) all over the explored $\tan\beta$. To this end we choose the soft-SUSY-breaking masses and trilinear couplings as input parameters, so that they reproduce the masses and angles of (50), that is we adjust the values of the parameters in the sfermion mass matrices (3) as follows

$$\begin{aligned}
M_{\tilde{q}_L} &= M_{\tilde{d}_R} = M_{\tilde{b}_L} = 300 \text{ GeV} , & M_{\tilde{u}_R} &= 292 \text{ GeV} , & M_{\tilde{b}_R} &= 299 \text{ GeV} , & M_{\tilde{t}_R} &= 274 \text{ GeV} , \\
M_{\tilde{l}_L} &= 302 \text{ GeV} , & M_{\tilde{\tau}_R} &= 297 \text{ GeV} , \\
A_d &= A_b = A_l = 600 \text{ GeV} , & A_u &= 37.5 \text{ GeV} , & A_t &= -78 \text{ GeV} ,
\end{aligned}
\tag{52}$$

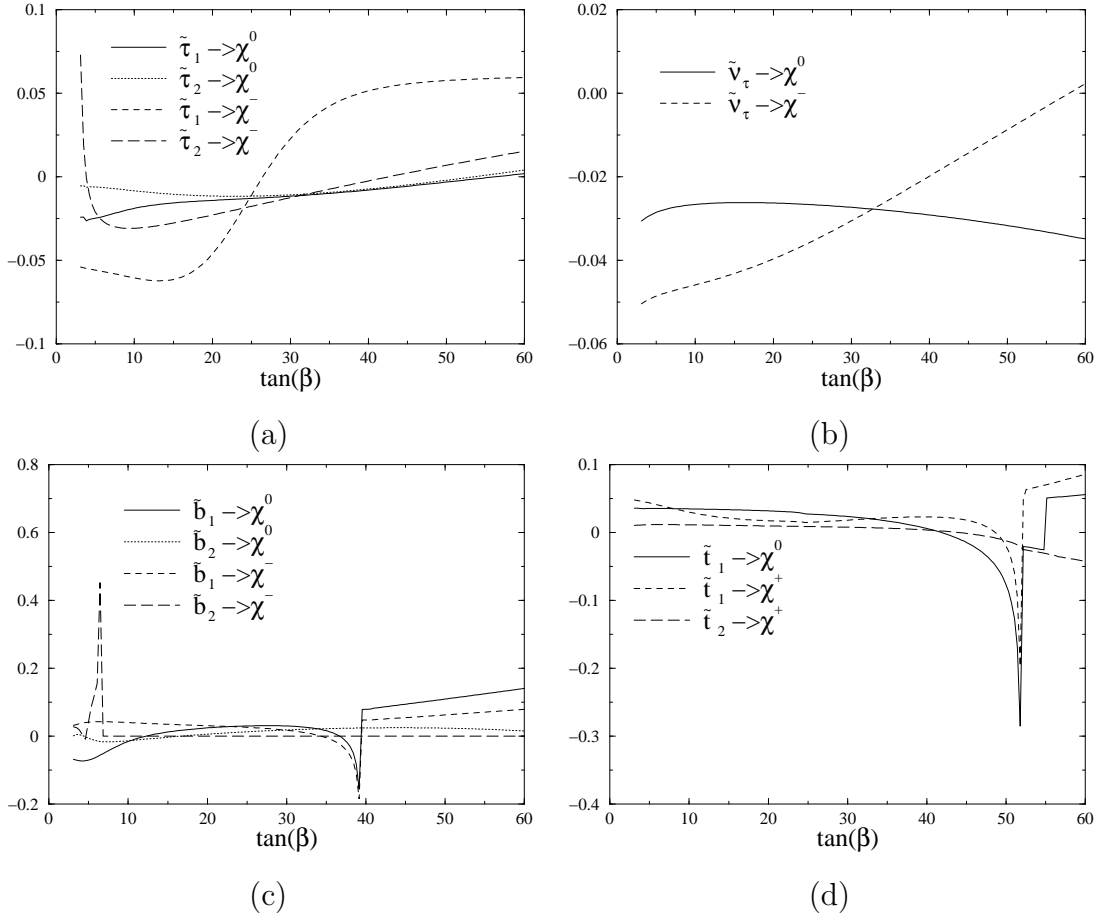


Figure 17: Non-universal corrections to the partial decay width of third generation sfermions into charginos and neutralinos, as a function of $\tan\beta$, with the soft-SUSY-breaking mass parameters fixed as in eq. (52).

with a common value for first and second generation squarks ($q \equiv u, d, s, c$, $u \equiv u, c$, $d \equiv d, s$), and for all sleptons ($l \equiv e, \mu, \tau$). The rest of the parameters are set as in eq. (50) (viz. $\mu = 150$ GeV, $M = 250$ GeV, $M_{H^\pm} = 120$ GeV). By choosing this parameter set, the masses and mixing angles will change with $\tan\beta$. In Fig. 17 we show the corrections to the third generation sfermion decays as a function of $\tan\beta$. We see that a large value of $\tan\beta$ may increase the absolute value of the corrections, but they stay below few ten percent for the allowed range $\tan\beta < 60$.

3.3 QCD corrections and SUSY threshold effects

The QCD corrections to the partial decays widths of sfermion decays into charginos and neutralinos were computed in [11, 19]. We have performed an independent computation, and have verified the analytical and numerical results of Ref. [11]. We will need these

partial results to compute the full one-loop branching ratios of the sfermion decays.

The QCD corrections can be very large in certain parts of the parameter space. This applies especially for squarks decaying into higgsino-type charginos or neutralinos. These large corrections can be absorbed by an adequate resummation of the leading effects. The latter are of two types: the running of the light-quark masses up to the scale of the sfermion masses produces large negative corrections; the finite SUSY threshold corrections to the bottom-quark Yukawa coupling can also be large; they grow with $\tan\beta$, and its sign is opposite to μ – see the extensive literature [13, 9, 43, 44] on the subject. The authors of Ref. [44] demonstrated that, for the case of $H^+t\bar{b}$ coupling, these corrections can be exactly resummed to all orders of perturbation theory by using the effective bottom quark Yukawa coupling according to

$$h_b^{eff} \equiv \frac{m_b^{eff}}{v_1} \equiv \frac{m_b(Q)}{v_1(1 + \Delta_b)} , \quad (53)$$

where $m_b(Q)$ is the running quark mass, and Δ_b is the finite threshold correction.

By using the effective bottom quark mass in eq. (53) we are able to absorb a large part of the corrections into the effective couplings, yielding an improved partial decay width

$$\Gamma^{imp} \equiv \Gamma^0(m_b^{eff}) + (\Gamma^{1-loop} - \Gamma^{1-expans}) \equiv \Gamma^0(m_b^{eff})(1 + \delta^{rem}) , \quad (54)$$

where $\Gamma^{1-expans}$ is the one-loop expansion of $\Gamma^0(m_b^{eff})$. The previous equation defines the *remainder* of the one-loop contributions, namely what is left after subtracting the one-loop part of the resummed threshold corrections from the full one-loop result. It reads

$$\delta^{rem} = \frac{\Gamma^{1-loop} - \Gamma^{expand}}{\Gamma^0(m_b^{eff})} . \quad (55)$$

The improved QCD correction factor is then given by

$$\delta^{imp-QCD} = \frac{\Gamma^{imp} - \Gamma^0(m_b)}{\Gamma^0(m_b)} . \quad (56)$$

In Fig. 18 we show an example. We have plotted the one-loop and the improved QCD corrections to the bottom-squark partial decay widths into neutralinos as a function of $\tan\beta$, using the input parameters (52) and a gluino mass $m_{\tilde{g}} = 500$ GeV. The strong coupling constant is evaluated at the mass scale of the decaying particle, using the normalization $\alpha_S(M_Z) = 0.12$. The growing in absolute value of the one-loop QCD corrections is due to the increase of the bottom-squark mass splitting (entering Δ_b) with $\tan\beta$. For $\tan\beta \gtrsim 25$ they already pass the -100% value. On the other hand δ^{rem} is well behaved in all the $\tan\beta$ range, and it is seen not to be negligible at all in some cases.

The large negative corrections visible in Fig. 18 have a twofold origin. First, the running of the bottom quark mass provides large negative corrections due to *standard* QCD renormalization group effects. Second, the sign of the QCD contributions to the threshold corrections is opposite to that of μ (since $\Delta_b \propto \mu$ in eq. (53)). Therefore both kinds of contributions reinforce mutually in the originally chosen scenario $\mu > 0$. In the alternative

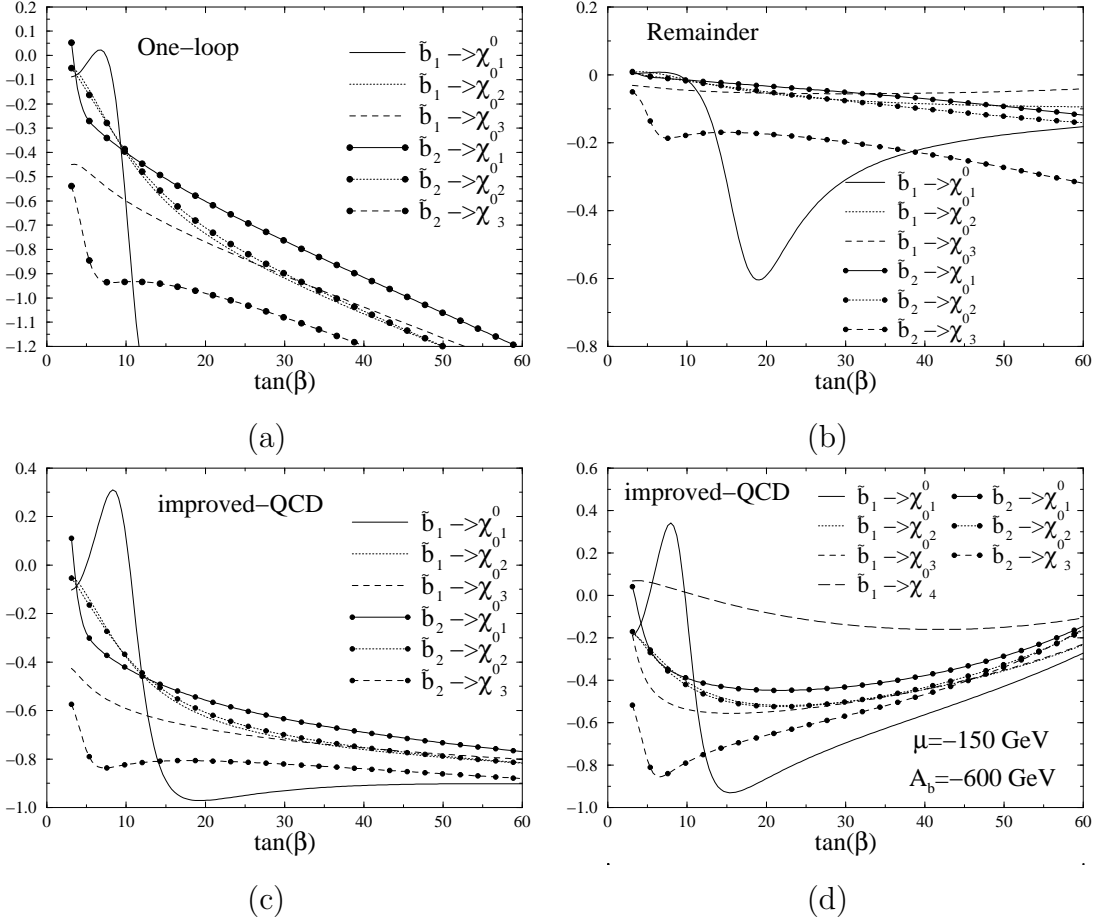


Figure 18: QCD corrections to the bottom-squark decays into neutralinos as a function of $\tan\beta$: **a)** one-loop corrections; **b)** remainder corrections – eq. (55); **c)** improved corrections – eq. (56). Parameters fixed as in eq. (52). **d)** improved corrections for the alternative $\mu < 0$ scenario, rest of parameters as in (52). Only those channels with a branching ratio larger than 10% are shown. The two lines corresponding to the χ_2^0 channels coincide visually.

scenario ($\mu < 0$) the two contributions partially cancel each other, giving a smaller total (negative) correction. Thus in the $\mu < 0$ scenario the SUSY-QCD effects actually prevent the decay rates from being too much suppressed by the gluonic corrections.

One has to be careful in the use of the effective bottom-quark mass (53) in the case of positive corrections ($\mu < 0$), since in this case the effective Yukawa coupling grows and can become non-perturbative for large values of $|\mu|$ and $\tan\beta$. In Fig. 18d we show a scenario with $\mu < 0$. The input parameters are those of eq. (52), but changing the sign of μ and the soft-SUSY-breaking trilinear couplings A_f . Although the corrections are still negative, we clearly see the change of trend for large $\tan\beta \gtrsim 20$; from this point onwards the (positive) threshold corrections are comparable to the effects of the running bottom quark mass. At $\tan\beta \simeq 60$ the two leading contributions nearly compensate each other, giving a total negative correction below 30%. So at large $\tan\beta$ some channels become essentially free of huge negative corrections, whereas in the original $\mu > 0$ scenario these channels were reduced by more than 70% due to quantum effects!

In Ref. [11] the numerical results for the QCD corrections to the partial sbottom decay widths were much smaller than those presented in Fig. 18. The reason is that in Ref. [11] the following set of parameters was used: a low value of $\tan\beta$ ($= 1.6$), small splitting between the two sbottom masses ($= 10$ GeV), and a small sbottom mixing angle ($\theta_b \simeq 0$). Under these conditions the SUSY threshold corrections to the bottom Yukawa coupling (Δ_b) are suppressed [9, 43, 44]. Moreover, the choice of $\mu < 0$ in Ref. [11] would mean that the finite threshold effects partially compensate for the renormalization group running of the bottom mass, thus decreasing the value of the corrections. At moderate or large values of $\tan\beta$ ($\gtrsim 10$), however, the rest of the conditions can not be fulfilled. If the sbottom mixing angle were small ($\theta_b \simeq 0$), then the soft-SUSY-breaking trilinear coupling would be large ($A_b \simeq \mu \tan\beta$), eventually spoiling the vacua condition (6). Even if one drops the condition (6), then the weak corrections would blow up due to the non-perturbativity of the Higgs-squark-squark trilinear coupling entering the three-point function corrections in Fig. 2. We conclude, therefore, that sticking to the necessary condition (6) provides a natural suppression of the Higgs-squark-squark trilinear coupling, while maintaining the perturbativity of the weak corrections over the whole $\tan\beta$ range. At the same time, it means that for $\tan\beta \gtrsim 10$ the two sbottom masses have significant splitting, and $\theta_b \neq 0$, providing large corrections due to the finite threshold effects.

We remark that whereas the finite threshold corrections (Δ_b) can be regarded as *non-decoupling* effects in the study of the Higgs sector of the MSSM, this is not so for the sfermion decays under consideration (even though we have kept the *non-decoupling* denomination also in our case). Indeed, the non-decoupling property applies when *all* the SUSY parameters (μ , A_b , $m_{\tilde{b}_a}$, $m_{\tilde{g}}$) are simultaneously scaled. However, being the sbottom quark mass itself the process energy, the scaling of the SUSY parameters entails a simultaneous scaling of the process energy, and therefore the Δ_b corrections cannot be considered here as genuine non-decoupling quantum effects. Moreover, in an scenario of large μ ($\mu \gg m_{\tilde{b}_a}$) the light chargino is basically a gaugino, and so its coupling to quarks and squarks is essentially a gauge coupling, not a Yukawa coupling. As a result the sbottom decay into light charginos/neutralinos is not sensitive to Δ_b in this limit.

3.4 Branching ratios

At the end of the day we analyze the higher-order effects on the branching ratios. Notice that in practice only the branching ratios are directly accessible from the measurements of the various cross-sections at the colliders. Therefore the $BR(\tilde{f} \rightarrow f'\chi)$ are the true observables in this kind of analysis, and we will compute them from the corresponding corrections to the partial decay widths that we have considered in the previous sections. In particular we have to include the QCD and the threshold effects. In the following analysis we also take into account the (generally small) effects of the shift of the masses in the phase-space factor. Specifically we show the following quantities:

- Tree-level branching ratio (BR^0);
- QCD-correction to the branching ratio as discussed in section 3.3, including the QCD corrections to the \tilde{t}_1 mass:

$$\Delta BR^{QCD}(\tilde{f} \rightarrow \chi) = \frac{\Gamma^{imp}(\tilde{f} \rightarrow \chi)}{\sum_{\chi_i^\pm, \chi_\alpha^0} \Gamma^{imp}(\tilde{f} \rightarrow \chi)} - BR^0(\tilde{f} \rightarrow \chi) \quad , \quad (57)$$

Γ^{imp} being defined in (54);

- Total correction to the branching ratios (QCD and EW), including the QCD and EW corrections to the \tilde{t}_1 mass, and the EW corrections to the neutralino masses

$$\Delta BR^{total}(\tilde{f} \rightarrow \chi) = \frac{\Gamma^{imp}(\tilde{f} \rightarrow \chi) + \Gamma^0(\tilde{f} \rightarrow \chi)\delta(\tilde{f}_a \rightarrow f'\chi)}{\sum_{\chi_i^\pm, \chi_\alpha^0} (\Gamma^{imp}(\tilde{f} \rightarrow \chi) + \Gamma^0(\tilde{f} \rightarrow \chi)\delta(\tilde{f}_a \rightarrow f'\chi))} - BR^0(\tilde{f} \rightarrow \chi) \quad , \quad (58)$$

with $\delta(\tilde{f}_a \rightarrow f'\chi)$ as defined in (51).

The corrections to the branching ratios are usually smaller than those to the partial decay widths. The limiting case being when only one decay channel exists, and has obviously no corrections to the branching ratio.

Only results for the bottom- and top-squarks will be shown. The corrections to the slepton and first- and second-generation squarks are tiny, for two reasons: usually a single decay channel is dominant and the corrections to the partial decay widths are small. In addition the corrections will be shown only on those portions of the parameter space in which the only possible decay channels are the fermionic ones. The bosonic decay channels $\tilde{q}_a \rightarrow \tilde{q}'_b(V, H)$ can be dominant when they are open, and the quantum corrections to these channels must be taken into account to compute the corrections to the branching ratios [46].

In Fig. 19 we show the tree-level branching ratios of the bottom- and top-squarks as a function of the $SU(2)_L$ soft-SUSY-breaking gaugino mass parameter M , as well as the absolute corrections to the branching ratios of squarks decaying into neutralinos¹⁶.

¹⁶Since only two decay channels are open, the corresponding absolute corrections to the chargino branching ratio have the same absolute value and opposite sign.

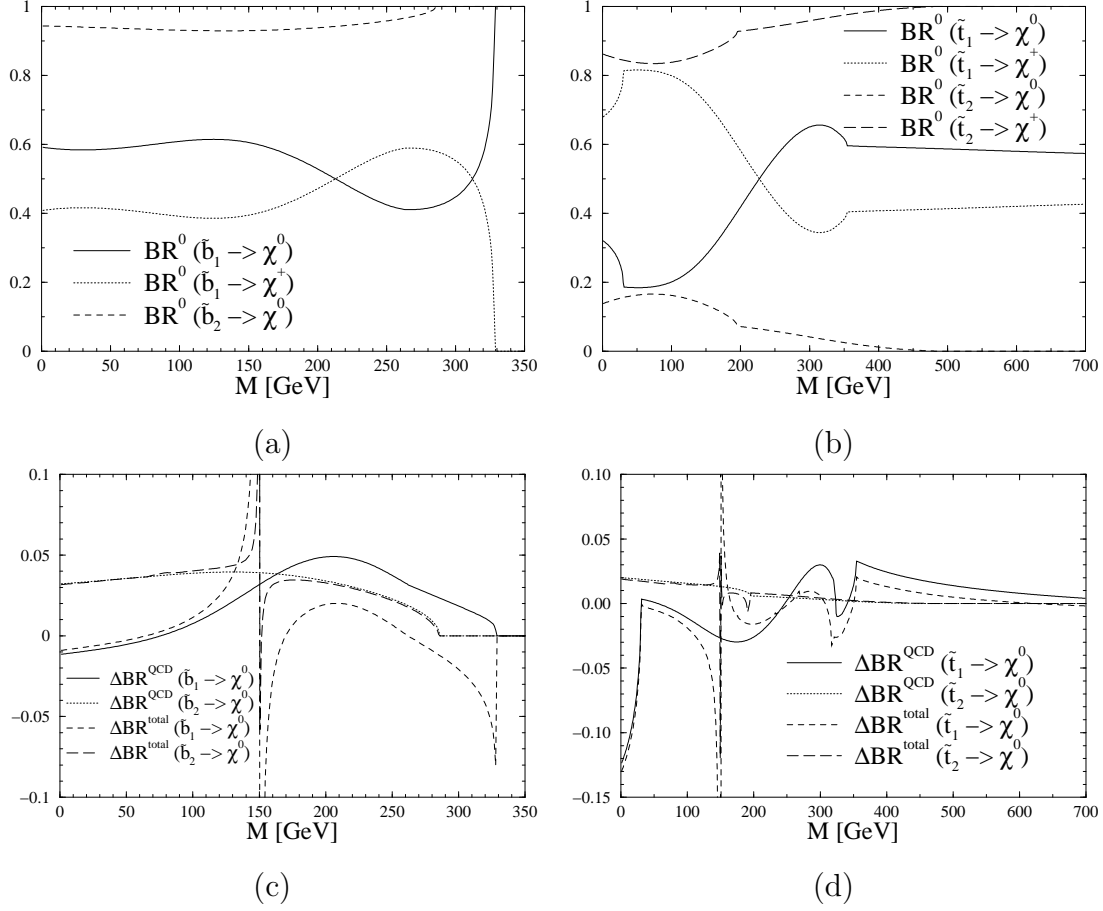


Figure 19: Tree-level branching ratios, **(a)-(b)**, and corrections to the branching ratios, **(c)-(d)**, of bottom- and top-squarks as a function of the soft-SUSY-breaking gaugino mass parameter M .

Although the QCD corrections are usually the largest ones, the EW and QCD corrections can be of the same order in certain scenarios. For example in Fig. 19c the QCD corrected $BR(\tilde{b}_1 \rightarrow b\chi^0)$ is $\sim 5\%$ larger than the tree-level one for $M \sim 200 - 250$ GeV, but the EW corrections compensate most of this correction, and the final correction is less than 1%.

The effects of the mass-shifts are in general very small, except near the threshold regions, where a given channel is permitted according to the tree-level masses prediction, but it is closed when one uses the one-loop prediction for the masses. This is the case in Fig. 19d. The decay channel $\tilde{t}_1 \rightarrow b\chi_3^0$ is open up to $M \simeq 354$ GeV according to the tree-level prediction for the heaviest top-squark mass. However the negative corrections to $m_{\tilde{t}_1}$ –table 1– enforce this channel to get closed for lighter M values, concretely, at $M \simeq 324$ GeV including only the QCD corrections and at $M \simeq 317$ GeV including the full corrections.

In Fig. 20 we show the branching ratios and its corrections as a function of the lightest

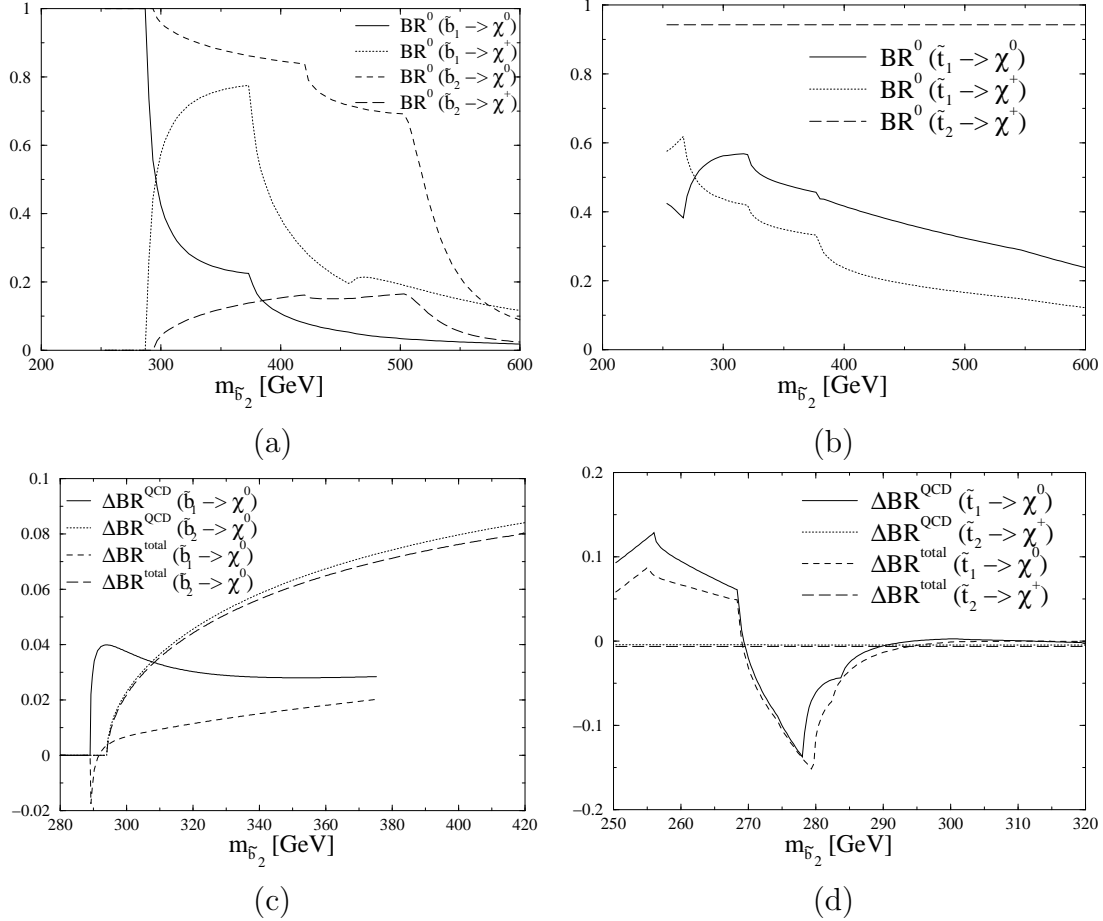


Figure 20: Tree-level branching ratios, **(a)-(b)**, and corrections to the branching ratios, **(c)-(d)**, of bottom- and top-squarks as a function of the lightest bottom-squark mass, maintaining $m_{\tilde{b}_1} = m_{\tilde{b}_2} + 5$ GeV.

bottom-squark mass (keeping the splitting between the two bottom-squarks at $m_{\tilde{b}_1} = m_{\tilde{b}_2} + 5$ GeV). The lines representing the corrections end at the points where the bosonic decay channels open. We see again that the EW corrections to the \tilde{b}_1 branching ratio can be of the same order as the QCD ones. For $m_{\tilde{b}_2} \lesssim 320$ GeV the 3–4% QCD contributions are almost compensated by the EW ones. For the \tilde{b}_2 , the EW corrections represent a small shift to the QCD-corrected branching ratios. For the top-squark the QCD corrections can be larger ($\gtrsim 10\%$), and the branching ratio also suffers an important shift from the EW sector.

The effects of the mixing angles are shown in Fig. 21. The corrections to the bottom-squark branching ratio show a simple structure. The corrections from the weak sector are comparable to that of the QCD sector for practically any value of the mixing angle. The \tilde{t} branching ratios and corrections are shown in Figs. 21b and d. The effect of the EW

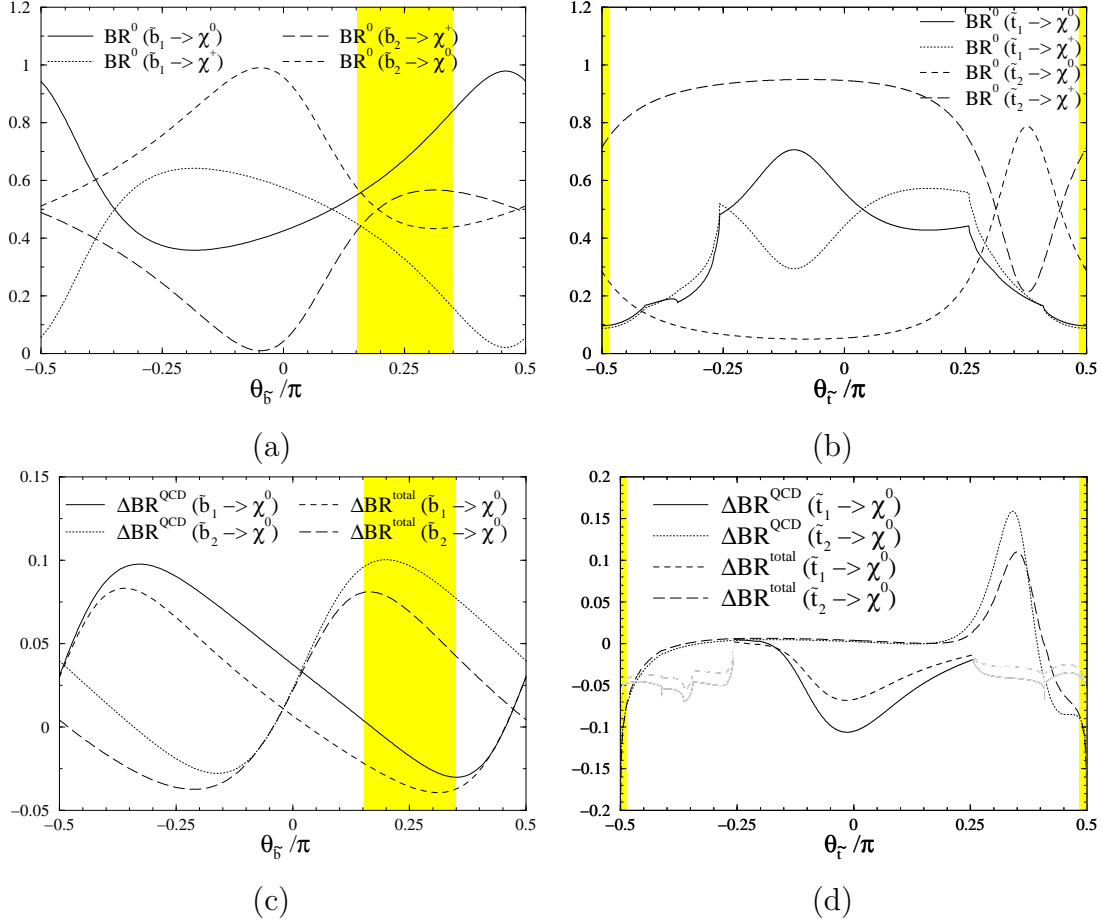


Figure 21: Tree-level branching ratios, **(a)**-**(b)**, and corrections to the branching ratios, **(c)**-**(d)**, of bottom- and top-squarks as a function of the respective mixing angles. The shaded regions correspond to the violation of the condition (6).

corrections is clearly visible above the QCD-corrected branching ratios.

We come finally to analyze the $\tan\beta$ dependence, which is shown in Fig. 22. In this case we will use again the soft-SUSY-breaking mass parameters in eq. (52) to compute the physical masses and mixing angles in the sfermion sector. The main effect of $\tan\beta$ on the tree-level branching ratios is due to the change in the sfermion masses themselves, providing the opening of the bosonic channels. Again, the weak corrections to the bottom-squark branching ratios are seen to be a tiny addition to the QCD induced ones. Opposite to that, the weak corrections to the top-squark decay branching ratios are larger, especially in the lightest top-squark channels. In this case they can be comparable to the QCD induced corrections.

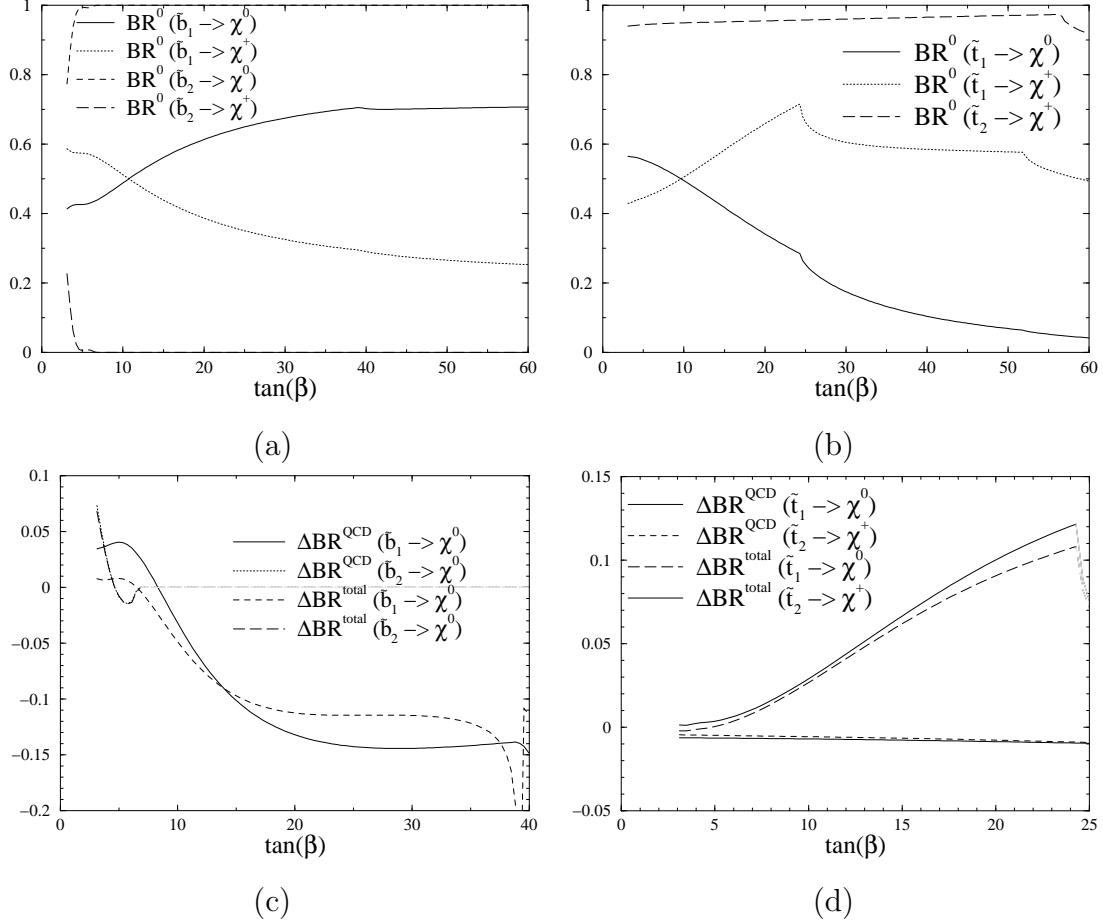


Figure 22: Tree-level branching ratios, **(a)**-**(b)**, and corrections to the branching ratios, **(c)**-**(d)**, of bottom- and top-squarks as a function of $\tan\beta$.

4 Conclusions

We have presented a consistent and complete one-loop on-shell renormalization scheme for the sfermion and the chargino-neutralino sectors of the MSSM. This scheme is suitable for the computation of one-loop electroweak corrections to observables relevant to the next generation of colliders.

We have applied this scheme to compute the full electroweak corrections to the partial decay widths of sfermions into charginos and neutralinos.

As a summary of the results we show in Table 3 the corrected branching ratios for all possible individual sfermion decays for the (low $\tan\beta$) input parameter set (50). For squarks we show both: the branching ratio including only QCD effects, and the fully corrected branching ratio. One can compare these results with the former tree-level results

	χ_1^0	χ_2^0	χ_3^0	χ_4^0	χ_1^+	χ_2^+
$BR^{total}(\tilde{\nu} \rightarrow l\chi)$	0.438	-	0.017	0.001	0.541	0.003
$BR^{total}(\tilde{e}_1 \rightarrow l\chi)$	0.017	0.621	0.003	0.010	0.319	0.030
$BR^{total}(\tilde{e}_2 \rightarrow l\chi)$	0.551	0.443	0.006	-	-	-
$BR^{total}(\tilde{\nu}_\tau \rightarrow l\chi)$	0.435	-	0.017	0.001	0.544	0.003
$BR^{total}(\tilde{\tau}_1 \rightarrow l\chi)$	0.021	0.617	0.006	0.010	0.316	0.030
$BR^{total}(\tilde{\tau}_2 \rightarrow l\chi)$	0.547	0.439	0.008	-	0.006	-
$BR^{QCD}(\tilde{u}_1 \rightarrow q\chi)$	0.026	0.258	0.007	0.002	0.703	0.004
$BR^{total}(\tilde{u}_1 \rightarrow q\chi)$	0.027	0.258	0.008	0.002	0.701	0.004
$BR^{QCD}(\tilde{u}_2 \rightarrow q\chi)$	0.579	0.416	0.005	-	-	-
$BR^{total}(\tilde{u}_2 \rightarrow q\chi)$	0.561	0.434	0.006	-	-	-
$BR^{QCD}(\tilde{d}_1 \rightarrow q\chi)$	0.314	0.106	0.020	0.020	0.490	0.048
$BR^{total}(\tilde{d}_1 \rightarrow q\chi)$	0.328	0.096	0.021	0.021	0.485	0.050
$BR^{QCD}(\tilde{d}_2 \rightarrow q\chi)$	0.571	0.424	0.005	-	-	-
$BR^{total}(\tilde{d}_2 \rightarrow q\chi)$	0.551	0.443	0.006	-	-	-
$BR^{QCD}(\tilde{t}_1 \rightarrow q\chi)$	0.164	0.257	0.144	-	0.099	0.335
$BR^{total}(\tilde{t}_1 \rightarrow q\chi)$	0.177	0.242	0.143	-	0.122	0.316
$BR^{QCD}(\tilde{t}_2 \rightarrow q\chi)$	0.063	-	-	-	0.937	-
$BR^{total}(\tilde{t}_2 \rightarrow q\chi)$	0.065	-	-	-	0.935	-
$BR^{QCD}(\tilde{b}_1 \rightarrow q\chi)$	0.308	0.104	0.031	0.018	0.538	-
$BR^{total}(\tilde{b}_1 \rightarrow q\chi)$	0.291	0.092	0.031	0.018	0.568	-
$BR^{QCD}(\tilde{b}_2 \rightarrow q\chi)$	0.541	0.386	0.054	-	0.019	-
$BR^{total}(\tilde{b}_2 \rightarrow q\chi)$	0.528	0.395	0.056	-	0.020	-

Table 3: Corrected branching ratios of sfermion decays into charginos and neutralinos for the parameter set (50). Branching ratios below 10^{-3} are not shown.

in Table 2 to assess the importance of the corrections in this particular parameter set¹⁷. A close comparison shows that, in fact, the EW corrections can have an effect as large as the QCD corrections alone. We can compare, for example, the leading branching ratio of the lightest up-squark ($\tilde{u}_2 \rightarrow u\chi_1^0$: $BR^0 = 58\%$, $BR^{QCD} = 57.9\%$, $BR^{total} = 56.1\%$) or the lightest sbottom ($\tilde{b}_2 \rightarrow b\chi_1^0$: $BR^0 = 50.2\%$, $BR^{QCD} = 54.1\%$, $BR^{total} = 52.8\%$).

The corrections show a rich and complicated structure when the MSSM parameters are varied. Nevertheless, we have been able to provide physical explanations of our results.

Indeed, we have identified sources of non-decoupling effects in these radiative corrections. In contradistinction to the Standard Model case, none of the MSSM particles decouples from these corrections¹⁸ – the non-decoupling effects being logarithmic in the heavy

¹⁷We have not searched for an *optimized* parameter set to enhance or decrease the value of the corrections, but just used *typical* values for the input parameters. The reader is warned that in other *typical* scenarios (e.g. large $\tan\beta$) the corrections may look much different, as we have shown in previous sections.

¹⁸This applies to supermultiplets in which one of the components is light, e.g. a SM particle. A super-

masses. As a consequence all particles of the MSSM must be taken into account in any computation involving loop diagrams with external fermion-sfermion-chargino/neutralino couplings. In some cases, however, the term multiplying this logarithm is small.

Furthermore, we have identified a class of universal corrections to the fermion-sfermion-chargino/neutralino couplings, that can be treated as *effective coupling matrices* for the chargino/neutralino sector. These universal corrections consist of the fermion-sfermion contributions to the self-energies of the gauge bosons, Higgs bosons, charginos and neutralinos. The *effective coupling matrices* absorb the non-decoupling effects of sfermions. Explicit analytic expressions for these corrections have been given in a simple example, but the general analysis has been performed numerically. These corrections can be large ($\sim 5 - 10\%$ for sfermion masses around 1 TeV) and grow logarithmically with the sfermion masses. A physical explanation of this effect using renormalization group arguments has been given.

The bulk of the non-universal corrections grow as a logarithm squared of the particle decay mass, due to the Sudakov-type double logarithms of the electroweak corrections.

For sfermion masses around 300 GeV, relevant for a 800 GeV e^+e^- linear collider such as TESLA, the non-universal electroweak corrections to the slepton and first- and second-generation squark partial decay widths are small. For top- and bottom-squarks the corrections are larger due to the large Yukawa couplings. The *threshold*-like corrections to the quark Yukawa couplings are important at large $\tan\beta$ for 3rd generation sfermions, and they must be resummed to obtain meaningful results.

The corrections remain always in the perturbative regime as long as the soft-SUSY-breaking trilinear couplings are not too large. This condition is, however, granted if the vacuum does not break the charge and/or colour symmetry. In particular, we point out that this vacuum condition cannot be preserved at large $\tan\beta$ by degenerating the sfermion masses and/or assuming vanishing sfermion mixing angles. Therefore, since $\mu = 0$ is phenomenologically ruled out, one can compensate the $\mu \tan\beta$ term in eq. (5) by an appropriate choice of the other parameters. For instance, at $\tan\beta = 30$ the vacuum condition can be preserved with the following set of masses and mixing angles: $m_{\tilde{b}} = (334, 268)$ GeV, $\theta_b \simeq -0.743$ $m_{\tilde{t}} = (356, 308)$ GeV and $\theta_t \simeq -0.576$.

The corrections can be significantly larger for individual decay channels that have small branching ratios. Therefore large corrections are washed out in the total decay widths $\Gamma(\tilde{f} \rightarrow f\chi^0)$ and $\Gamma(\tilde{f} \rightarrow f'\chi^\pm)$ – eq. (51).

We have combined the QCD corrections with the electroweak effects for the top- and bottom-squark partial decay widths, and have evaluated the full one-loop branching ratios of these supersymmetric particles in the case that the only open decay channels are the chargino/neutralino ones. In performing the computation of the corrections to the decay rates and branching ratios we have also taken into account the corrections to the squark and neutralino masses themselves. An specially interesting case appears when these mass shifts provide the opening (closing) of channels that would be closed (open) according to the naive tree-level prediction. Since the overall corrections can be very large for higgsino-multiplet in which all of the components are heavy will show decoupling properties.

type charginos/neutralinos, we have made use of the resummed expressions for the two leading quantum contributions to the bottom-quark Yukawa coupling, namely the running quark mass and the finite threshold supersymmetric effects.

The upshot of our analysis should be emphasized: the EW corrections can be of the same order of magnitude as the QCD effects, and therefore a consistent treatment of the sfermion decays beyond leading order in the MSSM demands to include the EW quantum contributions on the same footing as the QCD ones.

Acknowledgments

The calculations have been done using the QCM cluster of the DFG Forschergruppe “Quantenfeldtheorie, Computeralgebra und Monte-Carlo Simulation”. We are thankful to T. Hahn for his help regarding the Computer Algebra system. J.G. is thankful to D. Stöckinger, A. Vicini, G. Rodrigo, M. Melles and M. Spira for useful discussions. This collaboration is part of the network “Physics at Colliders” of the European Union under contract HPRN-CT-2000-00149. The work of J.G. is supported by the European Union under contract No. HPMF-CT-1999-00150. The work of J.S. has been supported in part by MECYT and FEDER under project FPA2001-3598.

References

- [1] J. Drees, talk at the *XX International Symposium on Lepton and Photon Interactions at High Energies*, Rome, Italy, 23rd-28th July 2001, [hep-ex/0110077](#); S. Mele, *Combined fit to the electroweak data and constraints on SM*, talk at the *International Europhysics Conference on High Energy Physics*, Budapest, Hungary, July 12-18, 2001; The LEP Collaborations, the LEP EW working group, the SLD Heavy flavour and Electroweak groups, *A combination of preliminary electroweak measurements and constraints on the standard model*, [hep-ex/0112021](#).
- [2] See e.g. M. Carena *et al.*, *Report of the Tevatron Higgs working group*, [hep-ph/0010338](#).
- [3] Atlas Collaboration, *Atlas Technical Design Report* CERN/LHCC/99-14/15; CMS Collaboration, *CMS Technical Proposal* CERN/LHCC/94-38; F. Gianotti, proceedings of the *IVth International Symposium on Radiative Corrections (RADCOR 98)*, p. 270, World Scientific 1999, ed. J. Solà.
- [4] *2nd Joint ECFA/DESY Study on Physics and Detectors for a Linear Electron-Positron Collider*, <http://www.desy.de/conferences/ecfa-desy-lc98.html>; *TESLA Technical Design Report* DESY 2001-011, Part III: *Physics at an e^+e^- Linear Collider*,

R. Heuer, D. Miller, F. Richard, P. Zerwas Editors, <http://tesla.desy.de/>,
hep-ph/0106315.

- [5] H. P. Nilles, *Phys. Rept.* **110** (1984) 1;
H. E. Haber, G. L. Kane, *Phys. Rept.* **117** (1985) 75;
A. B. Lahanas, D. V. Nanopoulos, *Phys. Rept.* **145** (1987) 1;
S. Ferrara, ed., *Supersymmetry*, vol. 1-2. North Holland/World Scientific, Singapore, 1987.
- [6] J. Solà, ed., *Quantum Effects in the MSSM*, World Scientific, 1998.
- [7] A. Dobado, M. J. Herrero, S. Peñaranda, *Eur. Phys. J.* **C7** (1999) 313,
hep-ph/9710313; *ibid.* **C12** (2000) 673, hep-ph/9903211; *ibid.* **C17** (2000) 487,
hep-ph/0002134.
- [8] M. Carena, M. Quirós, C. E. M. Wagner, *Nucl. Phys.* **B461** (1996) 407,
hep-ph/9508343;
H. E. Haber, R. Hempfling, A. H. Hoang, *Z. Phys.* **C75** (1997) 539,
hep-ph/9609331;
S. Heinemeyer, W. Hollik, G. Weiglein, *Phys. Rev.* **D58** (1998) 091701,
hep-ph/9803277; *Phys. Lett.* **B440** (1998) 296, hep-ph/9807423; *Eur. Phys. J.* **C9**
(1999) 343, hep-ph/9812472;
J. R. Espinosa, R. Zhang, *JHEP* **0003** (2000) 026, hep-ph/9912236; *Nucl. Phys.*
B586 (2000) 3, hep-ph/0003246;
M. Carena *et al.*, *Nucl. Phys.* **B580** (2000) 29, hep-ph/0001002;
G. Degrossi, P. Slavich, F. Zwirner, *Nucl. Phys.* **B611** (2001) 403, hep-ph/0105096.
- [9] L.J. Hall, R. Rattazzi, U. Sarid, *Phys. Rev.* **D50** (1994) 7048, hep-ph/9306309;
M. Carena, M. Olechowski, S. Pokorski, C.E.M. Wagner, *Nucl. Phys.* **B426** (1994)
269, hep-ph/9402253;
- [10] K. Hikasa, Y. Nakamura, *Z. Phys.* **C70** (1996) 139, *Erratum: ibid.* **C71** (1996) 356,
hep-ph/9501382.
- [11] A. Djouadi, W. Hollik, C. Jünger, *Phys. Rev.* **D55** (1997) 6975, hep-ph/9609419.
- [12] E. Katz, L. Randall, S. Su, *Nucl. Phys.* **B536** (1998) 3, hep-ph/9801416.
- [13] J. A. Coarasa *et al.*, *Eur. Phys. J.* **C2** (1998) 373, hep-ph/9607485.
- [14] J. A. Coarasa *et al.*, *Phys. Lett.* **B425** (1998) 329, hep-ph/9711472;
J. Guasch, R. A. Jiménez, J. Solà, *Phys. Lett.* **B360** (1995) 47, hep-ph/9507461;
J. A. Coarasa, R. A. Jiménez, J. Solà, *Phys. Lett.* **B389** (1996) 312,
hep-ph/9511402.
- [15] A. Belyaev, D. Garcia, J. Guasch, J. Solà, *Phys. Rev.* **D65** (2002) 031701,
hep-ph/0105053; *ibid.* *JHEP* **0206** (2002) 059, hep-ph/0203031.

- [16] M. Berggren, R. Keränen, H. Nowak, A. Sopczak, proceedings of *International Workshop on Linear Colliders (LCWS 99)*, Sitges, Barcelona, Spain, 28 Apr - 5 May 1999, Universitat Autònoma de Barcelona 2000, eds. E. Fernández, A. Pacheco, hep-ph/9911345.
- [17] W. Beenakker, R. Höpker, M. Spira, P. M. Zerwas, *Nucl. Phys.* **B492** (1997) 51, hep-ph/9610490;
W. Beenakker *et al.*, *Nucl. Phys.* **B515** (1998) 3, hep-ph/9710451;
T. Plehn, *Phys. Lett.* **B488** (2000) 359, hep-ph/0006182.
- [18] H. Eberl, A. Bartl, W. Majerotto, *Nucl. Phys.* **B472** (1996) 481, hep-ph/9603206;
H. Eberl, S. Kraml, W. Majerotto, *JHEP* **05** (1999) 016, hep-ph/9903413.
- [19] S. Kraml *et al.*, *Phys. Lett.* **B386** (1996) 175, hep-ph/9605412.
- [20] W. Beenakker, R. Hopker, T. Plehn, P. M. Zerwas, *Z. Phys.* **C75** (1997) 349, hep-ph/9610313.
- [21] J. Guasch, W. Hollik, J. Solà, *Phys. Lett.* **B437** (1998) 88, hep-ph/9802329.
- [22] J. Guasch, W. Hollik, J. Solà, contribution to the *2nd Joint ECFA/DESY Study on Physics and Detectors for a Linear Electron-Positron Collider*, p.565, R. Heuer, F. Richard and P. Zerwas editors, LC-TH-2000-013, hep-ph/0001254.
- [23] J. Guasch, W. Hollik, J. Solà, *Phys. Lett.* **B510** (2001) 211, hep-ph/0101086.
- [24] W. Siegel, *Phys. Lett.* **B84** (1979) 193.
For reviews see e.g. D.M. Capper, D.R.T. Jones, P. van Nieuwenhuizen, *Nucl. Phys.* **B167** (1980) 479;
I. Jack, D.R.T. Jones, in: *Perspectives on Supersymmetry*, World Scientific 1998, 149-167, ed. G.L. Kane, hep-ph/9707278.
- [25] W. Hollik, D. Stöckinger, *Eur. Phys. J.* **C20** (2001) 105, hep-ph/0103009.
- [26] M. Böhm, H. Spiesberger, W. Hollik, *Fortsch. Phys.* **34** (1986) 687;
W. Hollik, *Fortschr. Phys.* **38** (1990) 165.
- [27] P. Chankowski, S. Pokorski, J. Rosiek, *Nucl. Phys.* **B423** (1994) 437 hep-ph/9303309;
A. Dabelstein, *Z. Phys.* **C67** (1995) 495, hep-ph/9409375; *Nucl. Phys.* **B 456** (1995) 25, hep-ph/9503443;
- [28] H.E. Haber, R. Hempfling, *Phys. Rev. Lett.* **66** (1991) 1815;
Y. Okada, M. Yamaguchi, T. Yanagida, *Prog. Theor. Phys.* **85** (1991) 1;
J. Ellis, G. Ridolfi, F. Zwirner, *Phys. Lett.* **B257** (1991) 83; *ibid.* **B262** (1991) 477;
R. Barbieri, M. Frigeni, *Phys. Lett.* **B258** (1991) 395;
J.A. Bagger, K. Matchev, D.M. Pierce, R. Zhang, *Nucl. Phys.* **B491** (1997) 3, hep-ph/9606211.

- [29] A. Freitas, D. Stöckinger, [hep-ph/0205281](#).
- [30] J. M. Frère, D. R. T. Jones, S. Raby, *Nucl. Phys.* **B222** (1983) 11;
M. Claudson, L. J. Hall, I. Hinchliffe, *Nucl. Phys.* **B228** (1983) 501;
C. Kounnas, A. B. Lahanas, D. V. Nanopoulos, M. Quirós, *Nucl. Phys.* **B236** (1984) 438;
J. F. Gunion, H. E. Haber, M. Sher, *Nucl. Phys.* **B306** (1988) 1.
- [31] D. Pierce, A. Papadopoulos, *Phys. Rev.* **D50** (1994) 565, [hep-ph/9312248](#);
Nucl. Phys. **B430** (1994) 278, [hep-ph/9403240](#).
- [32] J. Guasch, J. Solà, *Z. Phys.* **C74** (1997) 337, [hep-ph/9603441](#).
- [33] J. L. Kneur, G. Moultaka, *Phys. Rev.* **D59** (1999) 015005, [hep-ph/9807336](#);
Phys. Rev. **D61** (2000) 095003, [hep-ph/9907360](#);
S. Y. Choi *et al.*, *Eur. Phys. J.* **C14** (2000) 535, [hep-ph/0002033](#).
- [34] H. Eberl, M. Kincel, W. Majerotto, Y. Yamada, *Phys. Rev.* **D64** (2001) 115013,
[hep-ph/0104109](#).
- [35] T. Fritzsche, W. Hollik, *Eur. Phys. J. C* **24** (2002) 619, [hep-ph/0203159](#).
- [36] D. Garcia, J. Solà, *Mod. Phys. Lett.* **A9** (1994) 211;
P. H. Chankowski *et al.*, *Nucl. Phys.* **B417** (1994) 101.
- [37] J. Küblbeck, M. Böhm, A. Denner, *Comput. Phys. Commun.* **60** (1990) 165;
T. Hahn, *Comput. Phys. Commun.* **140** (2001) 418, [hep-ph/0012260](#);
T. Hahn, C. Schappacher, *Comput. Phys. Commun.* **143** (2002) 54,
[hep-ph/0105349](#).
- [38] T. Hahn, M. Pérez-Victoria, *Comput. Phys. Commun.* **118** (1999) 153,
[hep-ph/9807565](#);
T. Hahn, *FeynArts*, *FormCalc* and *LoopTools* user's guides, available from
<http://www.feynarts.de>;
G. J. van Oldenborgh, *Comput. Phys. Commun.* **66** (1991) 1.
- [39] M. A. Diaz, S. F. King, D. A. Ross, *Nucl. Phys.* **B529** (1998) 23 [hep-ph/9711307](#);
S. Kiyoura, M. M. Nojiri, D. M. Pierce, Y. Yamada, *Phys. Rev.* **D58** (1998) 075002
[hep-ph/9803210](#);
T. Blank, W. Hollik, [hep-ph/0011092](#).
- [40] D. E. Groom *et al.*, *Eur. Phys. J.* **C15** (2000) 1.
- [41] A. Sommerfeld: *Atombau und Spektrallinien*. Braunschweig: Vieweg, 1939.
- [42] A. D. Sakharov, *Zh. Eksp. Teor. Fiz.* **18** (1948) 631 [*Sov. Phys. Usp.* **34** (1991) 375].

- [43] D. M. Pierce, J. A. Bagger, K. Matchev, R. Zhang, *Nucl. Phys.* **B491** (1997) 3, hep-ph/9606211;
K. S. Babu, C. Kolda, *Phys. Lett.* **B451** (1999) 77, hep-ph/9811308;
F. Borzumati, G. R. Farrar, N. Polonsky, S. Thomas, *Nucl. Phys.* **B555** (1999) 53, hep-ph/9902443;
J. Guasch, W. Hollik, S. Peñaranda, *Phys. Lett.* **B515** (2001) 367, hep-ph/0106027.
- [44] M. Carena, D. Garcia, U. Nierste, C.E.M. Wagner, *Nucl. Phys.* **B577** (2000) 88, hep-ph/9912516.
- [45] P. Ciafaloni, D. Comelli, *Phys. Lett.* **B446** (1999) 278, hep-ph/9809321;
V. S. Fadin, L. N. Lipatov, A. D. Martin, M. Melles, *Phys. Rev.* **D61** (2000) 094002, hep-ph/9910338;
M. Beccaria, M. Melles, F. M. Renard, C. Verzegnassi, *Phys. Rev.* **D65** (2002) 093007, hep-ph/0112273.
- [46] A. Bartl *et al.*, *Phys. Lett.* **B435** (1998) 118, hep-ph/9804265;
A. Bartl *et al.*, *Phys. Lett.* **B419** (1998) 243, hep-ph/9710286; *Phys. Rev.* **D59** (1999) 115007;